CHAPTER 23

Erosion of Soils and Scour Problems

23.1 THE EROSION PHENOMENON

An erosion problem always has three components: the soil or rock, the water, and the geometry of the obstacle that the water is interacting with. The resistance of the soil or rock is characterized by its erodibility, the water action is quantified by its velocity, and the geometry of the obstacle is quantified by its dimensions. Background on erosion from Briaud (2008) appears in this chapter, including the associated case histories.

Figure 23.1 shows a free-body diagram of a soil particle, a cluster of particles, or a rock block at the bottom of a lake. The water imposes a normal stress (hydrostatic pressure) around the soil particle or rock block. The normal stress is slightly higher at the bottom than at the top because the bottom is slightly deeper in the water column. This normal stress difference creates the buoyancy force, which reduces the weight of the soil particle or rock block.

Figure 23.2 shows the same particle, cluster of particles, or rock block at the bottom of a flowing river. Three things happen when water starts flowing. First, a drag force and associated shear stresses develop at the interface between the soil particle or rock block and the water flowing over it. This drag force is very similar to the seepage force. Second, the normal stress on top of the soil particle or rock block decreases because of the water flow. Indeed, as the velocity increases around the particle or the obstacle, the pressure drops to maintain conservation of energy according to Bernoulli's principle. This phenomenon is similar to the air flow on top of an airplane wing where the pressure is lower than below the wing, thereby developing the uplift force necessary for the plane to fly. Third, the normal stresses and shear stresses applied at the boundaries fluctuate with time because of the turbulence in the water. These fluctuations find their roots in the appearance and disappearance of eddies, vortices, ejections, and sweeps in the flowing water; they can contribute significantly to the erosion process, especially at higher velocities. In some cases they are the main reason for erosion. The contribution of turbulence fluctuations to the erosion process has been studied by several authors, including Croad (1981), Raudkivi (1998), Hoffmans and Verheij (1997), Bollaert (2002), and Hofland et al. (2005). The combination of the mean value and the fluctuations around the mean of the drag force and uplift force can become large enough to pluck and drag the soil particle, soil particle cluster, or rock block away and generate erosion.

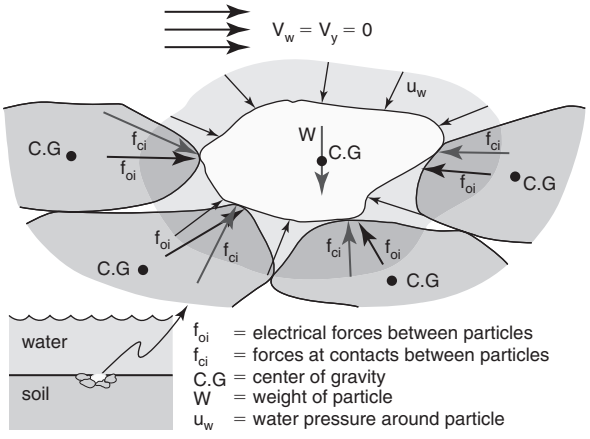

Figure 23.1 Free-body diagram of a soil particle or rock block for a no-flow condition (Briaud 2008).

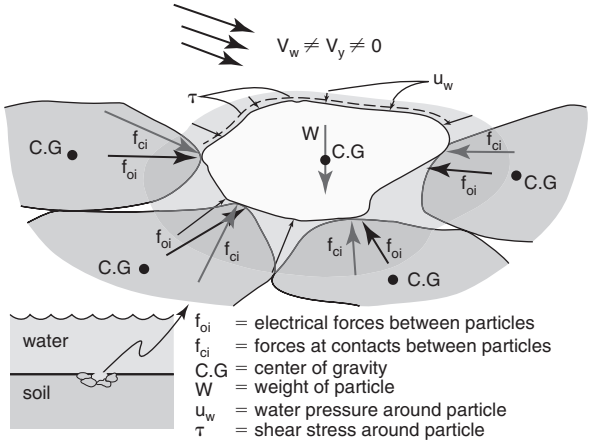

Figure 23.2 Free-body diagram of a soil particle or rock block when the water flows (Briaud 2008).

Geotechnical Engineering: Unsaturated and Saturated Soils Jean-Louis Briaud
© 2013 John Wiley & Sons, Inc. Published 2014 by John Wiley & Sons, Inc.

Note that in the case of unsaturated soils or saturated soils with water tension, the mechanical interparticle compressive forces (f_{ci} in Figures 23.1 and 23.2) can be significantly larger than in the case where the water is in compression. This apparent cohesion may increase the resistance to erosion, at least until the flow and presence of water destroy the water tension.

23.2 EROSION MODELS

The erodibility of a soil or rock can be defined as the relationship between the erosion rate $\dot{z}$ and the velocity of the water v near the soil-water interface. This definition is not very satisfactory because the velocity varies in direction and intensity in the flow field. In fact, strictly speaking, the water velocity is zero at the soil/rock-water interface. A more satisfactory definition is the relationship between the erosion rate $\dot{z}$ and the shear stress τ at the soil/rock-water interface:

$$\dot{z} = f(\tau) \tag{23.1}$$

The erosion function described by Eq. 23.1 represents the constitutive law of the soil or rock for erosion problems, much like a stress-strain curve represents the constitutive law of the soil or rock for a settlement problem. Although a definition based on shear stress is an improvement over a velocity-based definition, it is still not completely satisfactory, as shear stress is not the only stress that contributes to the erosion rate. A more complete description of the erosion function is given by Eq. 23.2:

$$\frac{\dot{z}}{u} = \alpha \left(\frac{\tau - \tau_c}{\rho u^2}\right)^m + \beta\left(\frac{\Delta\tau}{\rho u^2}\right)^n + \gamma\left(\frac{\Delta\sigma}{\rho u^2}\right)^p \tag{23.2}$$

where $\dot{z}$ is the erosion rate (m/s), u is the water velocity (m/s), τ is the hydraulic shear stress, τ_c is the threshold or critical shear stress below which no erosion occurs, ρ is the mass density of water (kg/m^3), $\Delta\tau$ is the turbulent fluctuation of the hydraulic shear stress, and $\Delta\sigma$ is the turbulent fluctuation of the net uplift normal stress.

All other quantities are parameters characterizing the soil being eroded. While this model is quite thorough, it is rather impractical at this time to determine the six parameters needed in Eq. 23.2 on a site-specific and routine basis. Today Eq. 23.3, which corresponds to the first term of Eq. 23.2, is widely accepted:

$$\frac{\dot{z}}{u} = \alpha \left(\frac{\tau - \tau_c}{\rho u^2}\right)^m \tag{23.3}$$

As additional fundamental work is performed in erosion engineering, it is likely that Eq. 23.3 will evolve toward Eq. 23.2.

23.3 MEASURING THE EROSION FUNCTION

In the early 1990s, an apparatus was developed to measure the erosion function. This erosion function apparatus (EFA) was described in detail in section 9.20.1, including the data reduction (Briaud et al. 2001a). The principle is to go to the site where erosion is being investigated, collect samples within the depth of concern, bring them back to the laboratory, and test them in the EFA. A 75 mm outside diameter sampling tube containing the sample is placed through the bottom of the conduit where water flows at a constant velocity (Figure 23.3). The soil or rock is pushed out of the sampling tube only as fast as it is eroded by the water flowing over it. For each velocity, an erosion rate is measured and a shear stress is calculated using Moody's chart (Moody 1944). Thus the erosion function is obtained point by point.

Examples of erosion functions are shown in Figure 23.4 for a fine sand and Figure 23.5 for a low-plasticity clay. Note that for the same average velocity of 1 m/s in the EFA test conduit, the rate of erosion for the sand is about 1000 times faster than for the clay. This indicates that the rate of erosion can be very different for different soils.

Other devices have also been developed to evaluate how resistant earth materials are to water flow. These include the rotating cylinder to measure the erosion properties of stiff soils

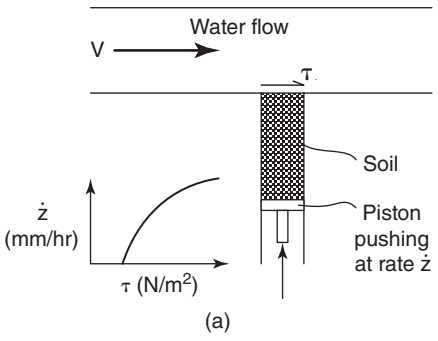

(b)

Figure 23.3 Erosion function apparatus to measure erodibility (Briaud et al. 1999).

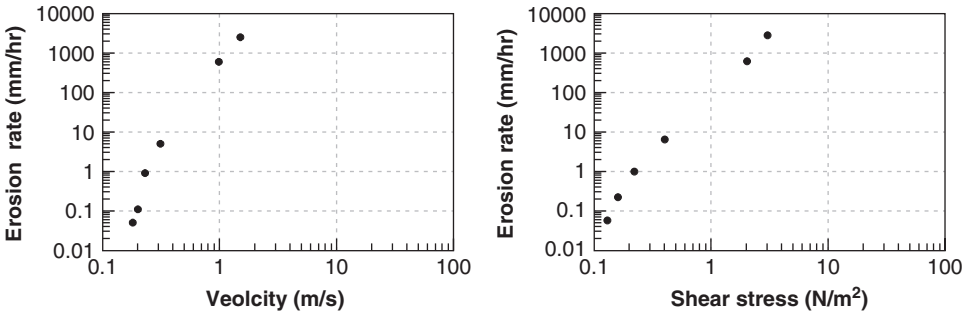

Figure 23.4 Erosion function for a fine sand as measured in the EFA.

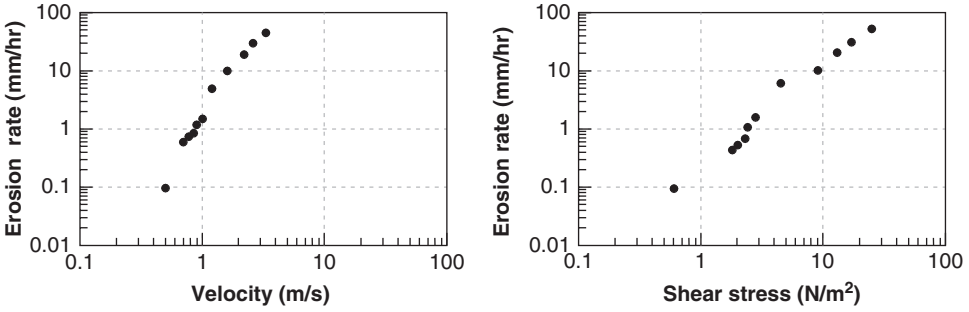

Figure 23.5 Erosion function for a low-plasticity clay as measured in the EFA.

(e.g., Chapuis and Gatien 1986), the jet test to evaluate the erodibility of soils (e.g., Hanson 1991), and the hole erosion test to measure the erosion properties of stiff soils (e.g., Wan and Fell 2004). More recently, a simple and inexpensive tool for field use has been developed called the pocket erodometer (Briaud et al. 2012). This tool is described in section 7.10. Tests with the pocket erodometer can be performed at the site on the end of a sample to get a first indication of the erodibility of the soil within minutes after sampling.

23.4 SOIL EROSION CATEGORIES

Categories are used in many fields of engineering: soil classification categories, hurricane strength categories, and earthquake magnitude categories, among others. Such categories have the advantage of quoting one number to represent a more complex condition. Erosion categories are proposed (Figure 23.6) to bring erodibility down in complexity from an erosion rate vs. shear stress function to a category number. Such a classification system can be presented in terms

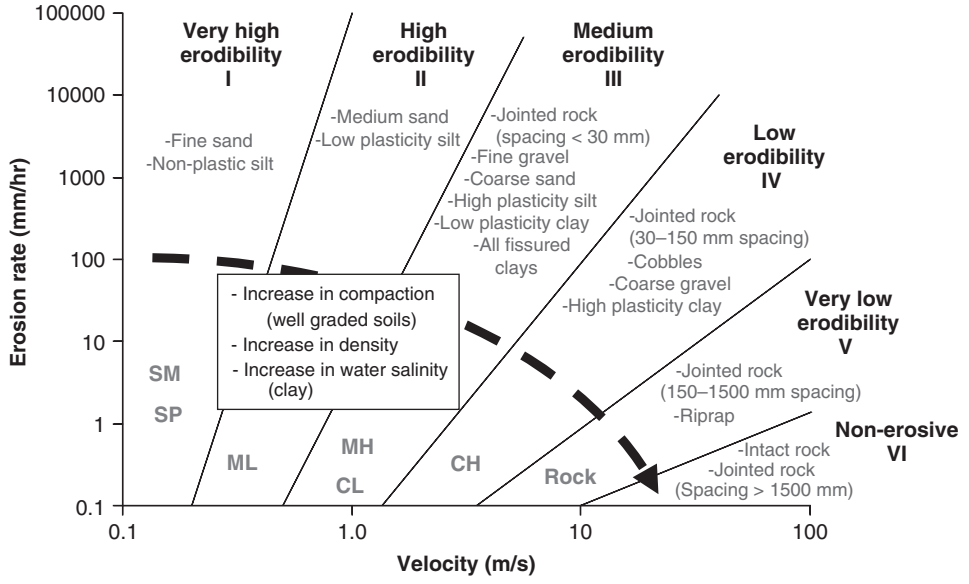

Figure 23.6 Proposed erosion categories for soils and rocks based on velocity.

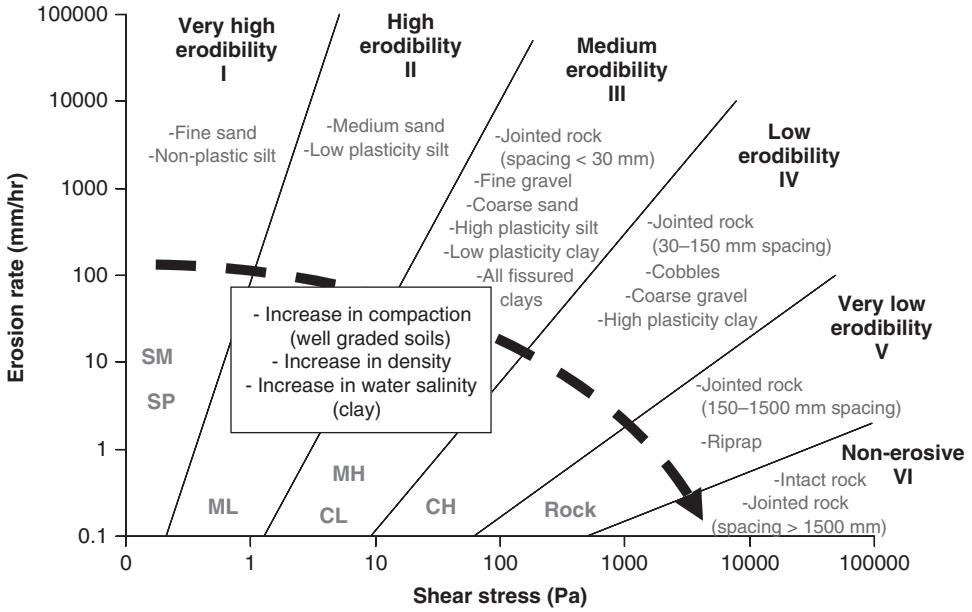

Figure 23.7 Proposed erosion categories for soils and rocks based on shear stress.

of velocity (Figure 23.6) or shear stress (Figure 23.7). The categories proposed are based on 20 years of erosion testing experience.

To classify a soil or rock, the erosion function is plotted on the category chart; the erodibility category number for the material tested is the number for the zone in which the erosion function fits. Note that, as discussed later, using the water velocity is less representative and leads to more uncertainty than using the shear stress; indeed, the velocity and the shear stress are not linked by a constant. The velocity chart has the advantage that it is easier to gauge a problem in terms of velocity. An erodibility classification chart developed on the basis of the pocket erodometer test is shown in Figure 7.30.

One of the most important soil parameters in erosion studies is the threshold of erosion. Below this threshold, erosion does not occur; above this threshold, erosion occurs. In terms of shear stress, this threshold is the critical shear stress τ_c; in terms of velocity, it is the critical velocity v_c. Figure 23.8 shows a plot of the critical velocity as a function of the mean grain size, and Figure 23.9 shows the same plot for the critical shear stress. The data come from measurements using the EFA as well as measurements published in the literature. As can be seen in Figures 23.8 and 23.9, the relationship between the critical value and the grain size has a V shape, indicating that the most erodible soils are fine sands with a mean grain size in the range of 0.1 to 0.5 mm. This V shape also points out that particle size controls the erosion threshold of coarse-grained soils, whereas particle size does not correlate with the erosion threshold of fine-grained soils. Note that Shields (1936) proposed a curve for coarse-grained soils in his doctoral work; his data are included in Figures 23.8 and 23.9. Shields's recommendations do not extend to fine-grained soils. Note also that Hjulstrom (1935) proposed such a curve for both coarse-grained soils and fine-grained soils, but his recommendations for fine-grained soils turned out to be too simple.

The erodibility of soils varies significantly from one soil to the next; therefore, erodibility depends on the soil properties. It depends also on the properties of the water flowing over the soil. For clays, the higher the salt concentration in the water, the more erosion-resistant the clay is (Cao et al. 2002; Croad 1981). The properties influencing erodibility are numerous; some of them are listed in Table 23.1. It appears reasonable to expect that a relationship would exist between common soil properties and erodibility—but erodibility is a function, not a number, so correlations can be made only with elements of that function, such as the critical shear stress or the initial slope of the erosion function. Such correlations have been attempted (Cao et al. 2002) and failed with very low coefficients of correlation. On the one hand, there should be a correlation; on the other hand, the correlation is complex and requires multiple parameters, all involved in the resistance of the soil to erosion. All in all, it is preferable to measure the erosion function directly with an apparatus such as the EFA.

23.5 ROCK EROSION

Soil erosion is not very well known, but rock erosion is even less known, so the engineer must exercise a great deal of engineering judgment when it comes to rock erosion. Nevertheless, many engineers and researchers have contributed to the advancement of knowledge in this relatively new field. They include Temple and Moore (1994), Annandale (1995), Kirsten et al. (1996), van Schalkwyk et al. (1995), Bollaert (2002), and Manso (2006).

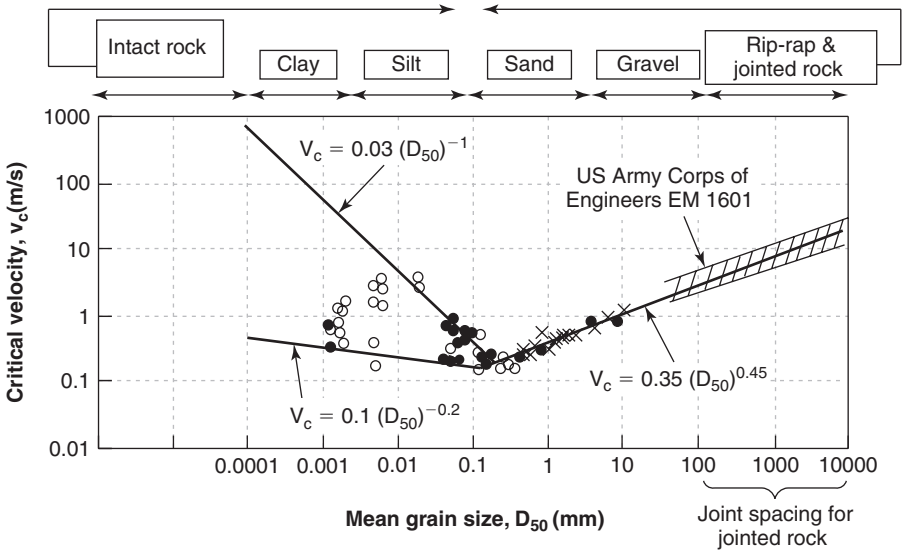

Legend:
- ● TAMU Data as reported by Briaud, J.-L. et. al. (2001). "Erosion Function Apparatus for Scour Rate Predictions." *J. Geotech. and Geoenvir. Engrg.,* ASCE, 127(2), 105–113.
- ○ TAMU Data as reported by Briaud, J.-L. (2006). "Erosion Tests on New Orleans Levee Samples." *Texas A&M University Internal Report.*
- x Data from Shields, Casey, US.WES, Gilbert, White as reported by Vanoni, V.A., ed. (1975). "Sedimentation Engineering." *ASCE manuals and reports on engineering practice,* ASCE, New York.

Figure 23.8 Critical velocity as a function of mean grain size.

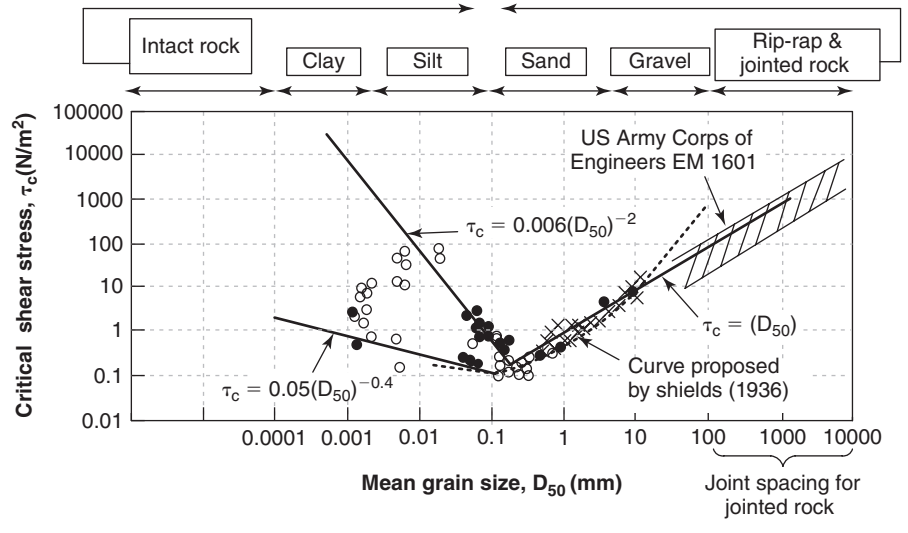

Legend:
- ● TAMU Data as reported by Briaud, J.-L. et. al. (2001). "Erosion Function Apparatus for Scour Rate Predictions." *J. Geotech. and Geoenvir. Engrg.,* ASCE, 127(2), 105–113.
- ○ TAMU Data as reported by Briaud, J.-L. (2006). "Erosion Tests on New Orleans Levee Samples." *Texas A&M University Internal Report.*
- x Data from Shields, Casey, US.WES, Gilbert, White as reported by Vanoni, V.A., ed. (1975). "Sedimentation Engineering." *ASCE manuals and reports on engineering practice,* ASCE, New York.

Figure 23.9 Critical shear stress as a function of mean grain size.

Table 23.1 Soil and Water Properties Influencing Erodibility

Soil water content	Soil clay minerals
Soil unit weight	Soil dispersion ratio
Soil plasticity index	Soil cation exchange cap
Soil undrained shear strength	Soil sodium absorption rate
Soil void ratio	Soil pH
Soil swell	Soil temperature
Soil mean grain size	Water temperature
Soil percent passing #200	Water salinity
	Water pH

Rock erodes through two main processes: rock substance erosion and rock mass erosion. *Rock substance erosion* refers to the erosion of the rock material itself, whereas *rock mass erosion* refers to the removal of rock blocks from the jointed rock mass. Rock substance erosion includes three submechanisms: erosion due to the hydraulic shear stress created by the water at the rock-water interface, erosion due to abrasion caused by sediments rubbing against the rock during the flow, and erosion from the impact of air bubbles that pit the rock surface due to cavitation at very high velocities. Rock mass erosion includes two submechanisms: erosion due to slaking, and erosion due to block removal between joints. Slaking can occur when a rock, such as a high-plasticity shale in an ephemeral stream, dries out and cracks during summer months; these small blocks are then removed by the next big flood. Block removal can occur if, during high-turbulence events, the difference in pressure between the top and the bottom of a rock block becomes large enough to overcome the weight and side friction on the block. Bollaert (2002) points out that brittle fracture and fatigue failure can contribute to breaking the rock into smaller pieces which are then carried away by the water. Note that most of the time, rock mass erosion will be the dominant process in rock erosion, with rock substance erosion occurring only rarely.

The critical velocity associated with rock erosion is much higher than the critical velocity associated with soil erosion in general. At the same time, the erosion rate for a given velocity is much lower for rock erosion than for soil erosion in general. Table 23.2 is an attempt at quantifying the critical velocity and the erosion rate of jointed rocks where rock mass erosion may control the process. This table is preliminary in nature and should be calibrated against field behavior. The critical velocities quoted in Table 23.2 refer to the velocity necessary to move a particle with a size equal to the spacing between joints; as such, they are likely lower bounds because they ignore any beneficial effect from the shear strength of the joints. Note that the orientation of the bedding of the rock mass is important, as shown in Figure 23.10. Engineering judgment must be used to increase or decrease the critical velocity when the bedding is favorable or unfavorable to the erosion resistance. In addition, it is highly recommended in all cases to measure the erosion function of the rock substance on core samples obtained from the site.

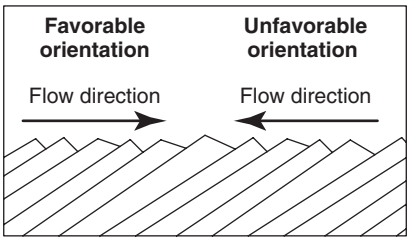

Figure 23.10 Effect of joint orientation on erosion resistance.

Examples of rock erosion rates can be collected from geology. For example, the Niagara Falls started about 12,000 years ago on the shores of Lake Erie, and have eroded back primarily through undercutting of the falls rock face to halfway between Lake Erie and Lake Ontario. This represents 11 km and an average rate of 0.1 mm/hr, through sandstones, shales, and limestone sedimentary rocks (http://en.wikipedia.org/wiki/Niagara_Falls). Another example is the Grand Canyon, where the Colorado River has generated 1600 m of vertical erosion through complex rock layers over an estimated 10 million years for an average rate of 0.00002 mm/hr (http://en.wikipedia.org/wiki/Geology_of_the_Grand_Canyon_area) as the Colorado Plateau was upheaving. These rates appear negligible at first glance, yet neglecting them would be to neglect the Grand Canyon or the

Table 23.2 Rock Mass Erosion

Joint Spacing (mm)	Critical Velocity (m/s)	Erosion Category	Orientation of Joints
<30	0.5–1.35	Category III Medium	Not applicable
30–150	1.35–3.5	Category IV Low	Evaluation needed
150–1500	3.5–10	Category V Very Low	Evaluation needed
>1500	>10	Category VI Nonerosive	Not applicable

Note: This table is preliminary in nature and should be calibrated against field behavior.

retreat of Niagara Falls. The lesson is clear: It is not only the rate of erosion that is important, but also the length of time over which that rate is applied.

23.6 WATER VELOCITY

Figure 23.11 shows the profile of water velocity as a function of flow depth. The water velocity is largest near the top of the water column and zero at the bottom. This has been measured repeatedly in hydraulic engineering. By comparison, the shear stress is highest at the bottom and near zero at the top of the water column. The relationship between the shear stress and the velocity can be established as follows. Because water is a Newtonian fluid, there is a linear relationship between the shear stress τ and the shear strain rate $d\gamma/dt$:

$$\tau = \mu \left(\frac{d\gamma}{dt} \right) \tag{23.4}$$

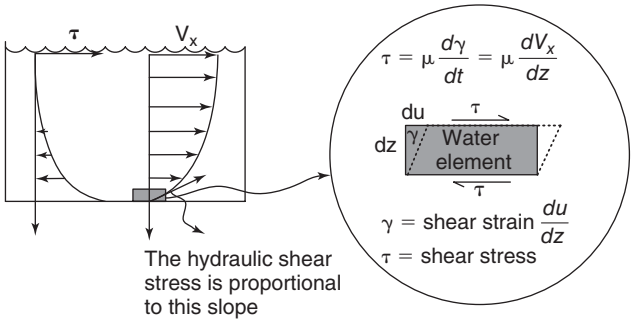

Figure 23.11 Velocity and shear stress profile versus flow depth.

where μ is the dynamic viscosity of the water (10^{-3} Pa.s at 20°C). This viscosity is different from the kinematic viscosity ν of water (10^{-6} m^2/s at 20°C) defined as $\nu = \mu/\rho$ where ρ is the mass density of water (1000 kg/m^3). Because, as shown in Figure 23.11, γ is du/dz, then dγ/dt is dv/dz where v and u are the water shear velocity and horizontal displacement at a depth z respectively. Then the shear stress τ at depth z is given by:

$$\tau = \mu \left(\frac{dv}{dz} \right) \tag{23.5}$$

Therefore, the shear stress is proportional to the gradient of the shear velocity profile with flow depth, and the shear stress at the soil/rock-water interface is the slope of the profile at the interface. If the slope of the water velocity profile at the water-soil or water-rock interface (*interface shear stress*) is kept constant, and if the water depth is varied, it can be shown that the mean depth velocity will vary as well. This implies that there is no constant ratio between mean depth velocity and interface shear stress. This is one reason why velocity alone is not as good a predictor of erosion as shear stress. Thus, any erosion design tool presented in terms of velocity should be used with caution. Nevertheless, velocity is much easier for the engineer to gauge than shear stress, and this is why both velocity and shear stress are used in practice.

The magnitude of these shear stresses is very small and measured in N/m^2. They are much smaller than the shear stresses that the geotechnical engineer is used to calculating in foundation engineering, for example, which are in the range of kN/m^2. Figure 23.12 gives examples of the range of shear stresses associated with various fields of engineering.

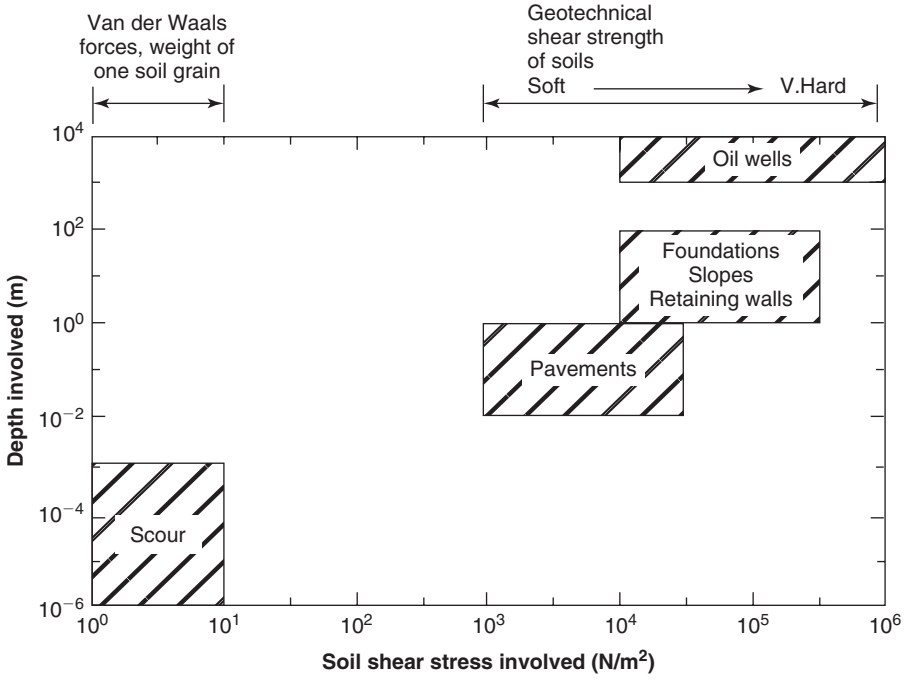

Figure 23.12 Range of shear stresses encountered in different engineering fields.

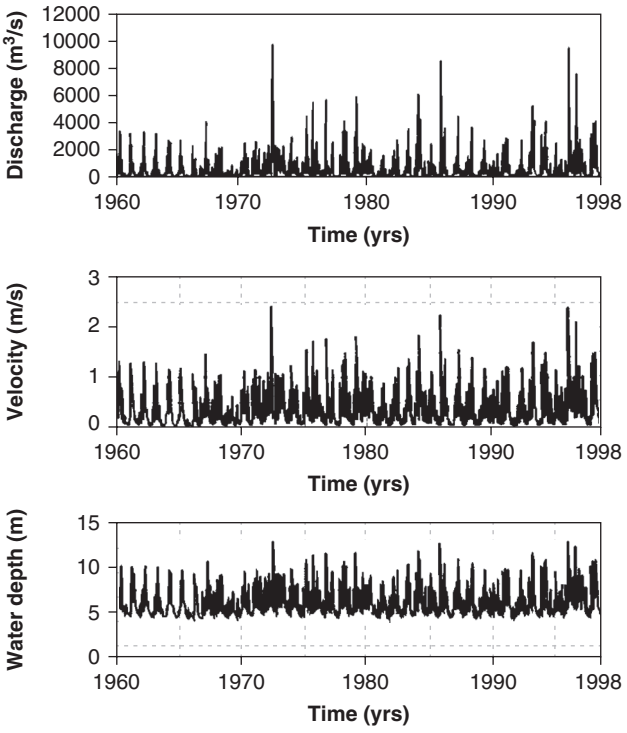

Figure 23.13 Discharge, velocity, and water depth hydrographs.

If the undrained shear strength is a reasonable measure of the strength of a clay for foundation engineering design, the critical shear stress is the "shear strength" of the same clay for erosion studies. The difference in magnitude of the stresses and the strengths between foundation engineering and erosion is that in erosion studies one looks at the resistance of one particle, or a small cluster of particles, whereas in foundation engineering one looks at the resistance of the soil mass associated with the scale of the foundation.

The water in a river does not flow at a constant velocity, so the velocity history over a period of time is a necessary input to many erosion problems. This velocity history or *hydrograph* is not usually readily available. Often, a discharge (m^3/s) hydrograph is available and must be transformed into a velocity (m/s) hydrograph and a water depth (m) hydrograph. This is commonly done by using software such as HEC-RAS (Brunner 2002). An example of the results of this transformation is shown in Figure 23.13. HEC-RAS solves the one-dimensional energy equation for gradually varied flow in natural or constructed channels and adds the one-dimensional momentum equation around hydraulic structures such as bridges, culverts, and weirs where the energy equation is no longer applicable.

The hydrograph can be used to determine the 100-year flood or the 500-year flood. One simple graphical method (e.g., Chow et al. 1988) consists of obtaining the yearly maximum flows from the hydrograph, ranking them in descending order of intensity, calculating for each flow the probability of exceedance as the rank divided by the total number of observations + 1, then plotting the flow versus the probability of exceedance on a semilog paper such as the one if Figure 23.14. Once the data are plotted, a linear regression is performed over, say, the first 20 to 30 years of data and extrapolated to the 0.01 probability of exceedance for the 100-year flood and to the 0.002 probability of exceedance for the 500-year flood. The return period is the inverse of the probability of exceedance. There are other and more refined ways of obtaining these design floods, but this simple graphical method helps one to understand the process and the meaning of a *100-year flood*: a flood that has a 1% chance of

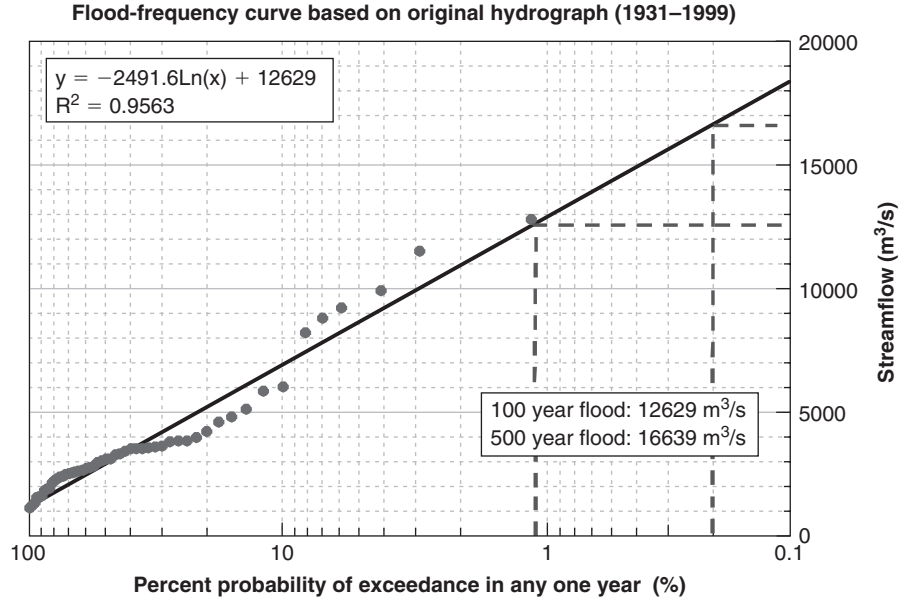

Figure 23.14 Flood frequency curve obtained from measured discharge hydrograph.

being exceeded in any one year. Figure 23.14 shows the result of an analysis for the hydrograph at the Woodrow Wilson bridge. As can be seen from that figure, the 100-year flood has a discharge of 12,600 m^3/s and the 500-year flood has a value of 16,600 m^3/s.

The probability of exceedance R of the design flood with a given return period T_r depends on the design life L_t of a structure:

$$R = 1 - (1 - 1/T_r)^{Lt} \tag{23.6}$$

If the design life of the bridge is 75 years, the probability that a flood with a return period of 100 years will be exceeded during the 75-year design life is 53%, according to Eq. 23.6; that probability is 14% for the 500-year flood. Only when one gets to the 10,000-year flood does the probability get lower than 1% (0.75%). Therefore, looking at those numbers alone, it seems desirable to use the 10,000-year flood for design purposes. This flood is used in design in the Netherlands for regions of the country deemed critical. The United States uses the 100- and 500-year floods for design purposes in hydraulic engineering; this leads to probabilities of exceedance in the tens of percent. By comparison, structural engineers use a probability of exceedance of about 0.1% for the design of bridge beams (LRFD target) and, judging from measured vs. predicted pile capacity databases (Briaud and Tucker 1988), geotechnical engineers use a probability of exceedance of the order of a few percent. While these numbers can be debated, it is relatively clear that these different fields of civil engineering operate at vastly different probability of exceedance levels. Note that risk is different from the probability of exceedance (see section 11.6.3), as it also involves the value of the consequence. Hence, the probability of exceedance target should vary with the consequence of the failure.

23.7 GEOMETRY OF THE OBSTACLE

The geometry of the obstacle encountered by the water influences the velocity of the water and the flow pattern, including turbulence intensity. When water approaches a pier in a river, it has to go around the pier. In doing so, it faces a restricted area and has to accelerate to maintain the flow rate. This acceleration results in a local mean depth velocity that can be 1.5 times higher than the approach mean depth velocity. If the approach velocity is lower than the critical velocity, but the local velocity around the pier reaches a value higher than the critical velocity, then *scour* occurs around the pier. This scour type is called *clear water scour*: that is, scour created by water that does not carry soil particles.

In contrast, if the approach velocity and the velocity around the pier are both higher than critical, then the scour type is *live bed scour*. This means that the water is carrying a significant amount of soil particles. The scour depth reached under live bed scour conditions is typically less than the scour depth reached under clear water scour conditions. The reason is that during live bed scour, some of the particles in suspension or rolling on the bottom fall down in the scour hole, thereby limiting the depth of the scour hole around the pier.

Figure 23.15*a* and *b* show results of numerical simulations of erosion created by water flow in a contracted channel. The CHEN 3D computer program (Chen et al. 1990; Chen 2002) was the program used.

23.8 BRIDGE SCOUR

Bridge scour refers to the erosion of the soil surrounding the foundation of bridge piers in rivers. The water flows at the approach velocity v, arrives at the bridge support, has to accelerate around that obstacle to maintain the flow rate, and thus has a higher potential to erode the river bottom around the foundation. Figure 23.16 shows the scour hole resulting from this erosion around a bridge pier. Bridge scour accounts for 60% of all bridge failures in the United States (Briaud 2006a). Figure 23.17 shows the progression of the scour depth as a function of time as a response to the flow history (hydrograph) at the bridge. It is important to know how deep the hole is going to be so that this scour depth can be ignored in the resistance of the foundation. The prediction of that scour depth requires knowledge of the soil erosion function, the water velocity, and the geometry of the obstacle. The obstacle can be a bridge pier, a bridge abutment, or the contraction of the river. As a result, we talk about pier scour, abutment scour, and contraction scour (Figure 23.18).

The simplest problem is that of a constant water velocity v flowing for an infinite time around a cylindrical pier of diameter B. Figure 23.19 shows a typical curve giving the scour depth as a function of time in this case. Experiments have shown that the scour depth z vs. time t curve is well described by a hyperbola:

$$z = \frac{t}{\dfrac{1}{\dot{z}_i} + \dfrac{t}{z_{\max}}} \tag{23.7}$$

where z is the scour depth, $\dot{z}_i$ is the initial erosion rate at a time equal to zero under a velocity v, $z_{\max}$ is the scour depth at a time equal to infinity (asymptotic value) under a velocity v, and t is the time during which the water has been flowing at the velocity v. The scour depth $z_{\max}$ is called the maximum scour depth under v and would occur if a flood creating v lasted a long time. If instead the flood last a finite amount of time, say 24 hours, then the scour depth is called the final scour depth z_{final} at the end of the flood event, say 24 hours. If $\dot{z}_i$ is large, then z_{final} will quickly approach $z_{\max}$, and one flood may be long enough to create $z_{\max}$. This is the case with very erodible soils, such as sands, where a maximum scour depth analysis called $z_{\max}$ analysis is sufficient. If, however, $\dot{z}_i$ is small, then z_{final} is likely to be much lower than $z_{\max}$ and it is economical to perform the more complex z_{final} analysis. This is the case with fine-grained soils.

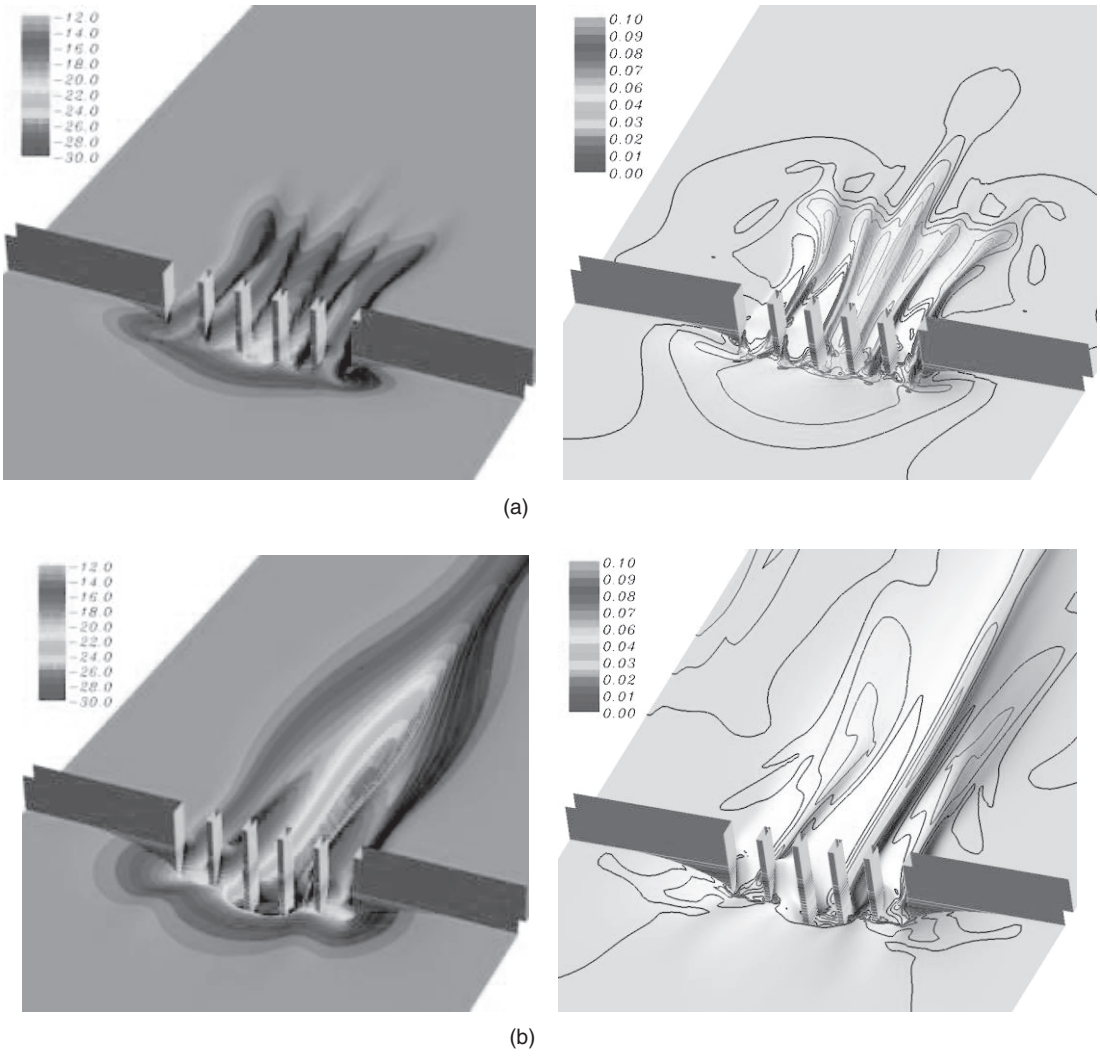

Figure 23.15 Predicted scour hole shape and streambed shear stresses around abutments and piers: *(a)* t = 2000 min. *(b)* t = 15,000 min. Scour depth and shear stress distributions at: *(a)* t = 2000 min and *(b)* t = 15,000 min. (From Chen 2002.)

Figure 23.16 Scour hole around bridge pier.

23.8.1 Maximum Scour Depth (z_{max}) Analysis

Pier Scour

The following equation gives the maximum scour depth for pier scour, that is to say the maximum depth of the hole that can form around the pier for a given set of parameters (Briaud 2012; Figure 23.18):

$$\frac{z_{\max(\text{Pier})}}{B'} = 2.2 \cdot K_{pw} \cdot K_{psh} \cdot K_{pa} \cdot K_{psp} \cdot (2.6 \cdot Fr_{(\text{pier})} - Fr_{c(\text{pier})})^{0.7} \tag{23.8}$$

where $z_{\max(\text{pier})}$ is the maximum depth of pier scour, B' is the projected width of the pier perpendicular to the flow, K_{pw} is the water depth influence factor for pier scour depth, K_{psh} is

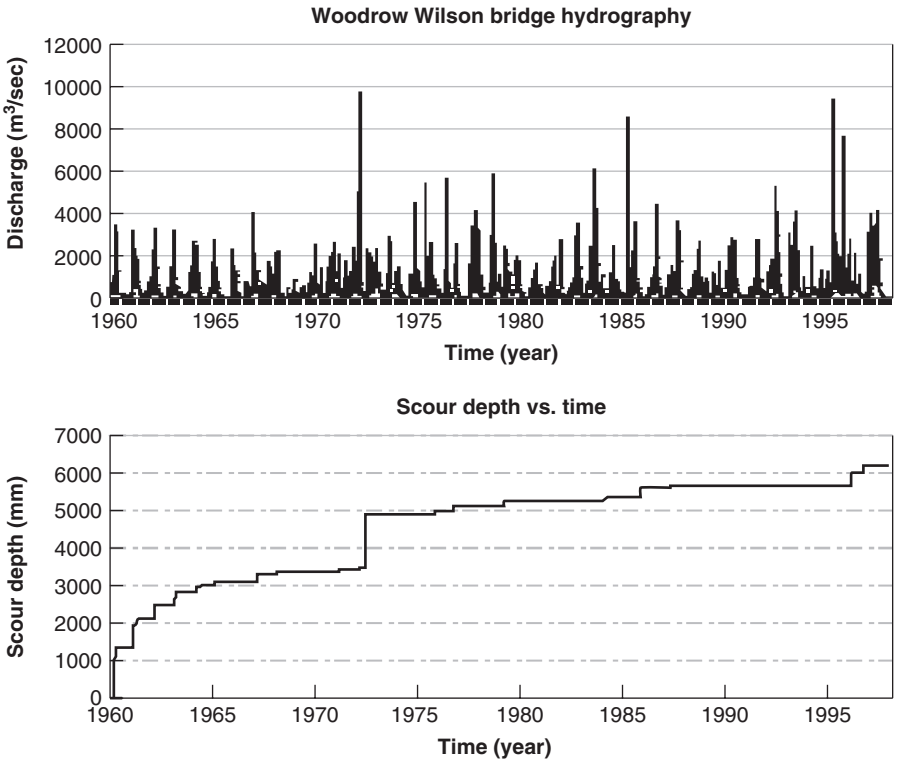

Figure 23.17 Increase in scour depth versus time as result of applied hydrograph.

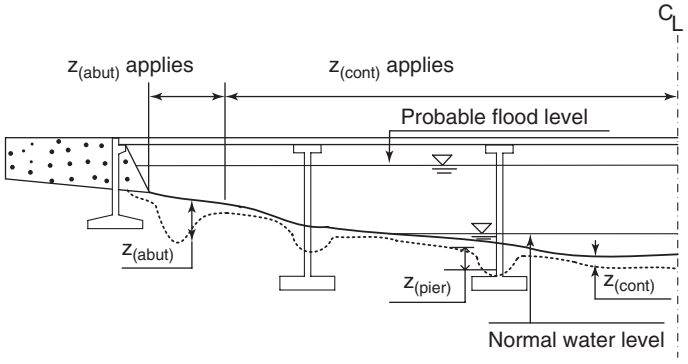

Figure 23.18 Pier scour, abutment scour, and contraction scour.

the pier shape influence factor for pier scour depth, K_{pa} is the aspect ratio influence factor for pier scour depth, the aspect ratio is L/B ratio of pier length L over pier width B, K_{psp} is the pier spacing influence factor for pier scour depth, $Fr_{(pier)}$ is the pier Froude Number (defined later) based on the approach velocity v_1 and pier width B', and $Fr_{c(pier)}$ is the critical pier Froude Number based on critical velocity v_c. The projected width B' (Figure 23.20) is given by:

$$B' = B\left(\cos\theta + \frac{L}{B}\cdot\sin\theta\right) \tag{23.9}$$

where B' is the projected width, B is the pier width, L is the pier length, and θ is the attack angle, which is the angle between the flow direction and the main direction of the pier.

The water depth influence factor K_{wa} corrects for the fact that the parenthetical expression on the right-hand side of Eq. 23.8 was developed for a pier in deep water. *Deep water* is defined as a water depth h_w larger than 1.43 B'. If the water depth is shallower than 1.43 B', the scour depth is reduced. The equation for K_{pw} is:

$$K_{pw} = \begin{cases} 0.89\left(\dfrac{h_w}{B'}\right)^{0.33}, & \text{for } \dfrac{h_w}{B'} < 1.43 \\ 1.0 \qquad\qquad\quad , & \text{else} \end{cases} \tag{23.10}$$

The pier shape influence factor K_{psh} is given in Table 23.3; it corrects for the fact that the parenthetical expression on the

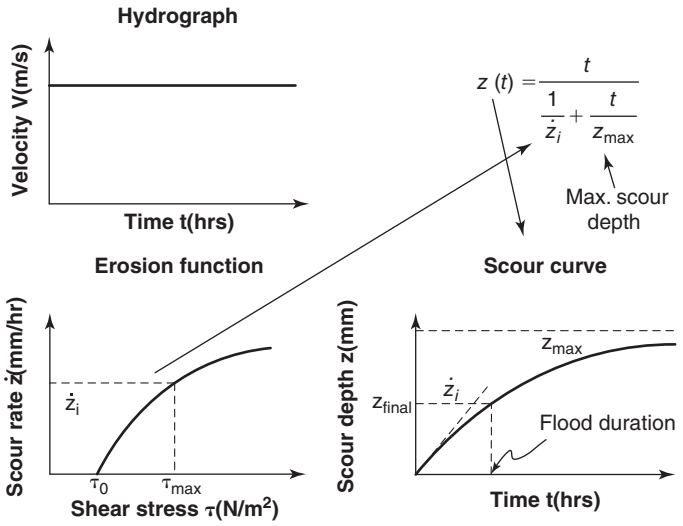

Figure 23.19 Scour depth vs. time curve for constant velocity.

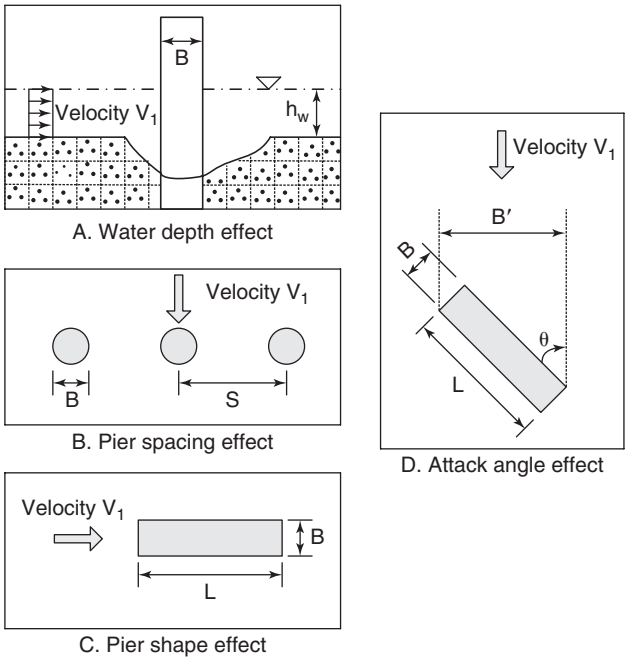

Figure 23.20 Definition of pier parameters.

right-hand side of Eq. 23.8 was developed for a cylindrical pier.

The aspect ratio influence factor K_{pa} corrects for the fact that the parenthetical expression on the right-hand side of Eq. 23.8 was developed for a cylindrical pier. This influence factor is taken care of by use of the projected width B' instead of B, so $K_{L/B}$ is always 1. The pier spacing influence factor K_{psp} corrects for the fact that the parenthetical expression on the right-hand side of Eq. 23.8 was developed for a single pier. If another pier is placed within the influence zone of the first one, the scour depth will be larger. The equation for K_{sp} is:

Table 23.3 Correction Factor for Pier Nose Shape (K_{psh})

Shape of Pier Nose	K_{psh}	Shape of Pier Nose	K_{psh}
Square nose	1.1	Circular cylinder	1.0
Round nose	1.0	Sharp nose	0.9

(Richardson Davis 2001)

$$K_{psp} = \begin{cases} 2.9\left(\frac{S}{B'}\right)^{-0.91}, & \text{for } \frac{S}{B'} < 3.42 \\ 1.0, & \text{else} \end{cases} \tag{23.11}$$

where S is the pier spacing and B' is the projected width. Equation 23.11 indicates that piers spaced more than 3.42 times the projected pier width from each other do not increase the scour depth at the pier. The pier Froude Number $Fr_{(\text{pier})}$ is given by:

$$Fr_{(\text{pier})} \left(= \frac{V_1}{\sqrt{g \cdot B'}}\right) \tag{23.12}$$

where V_1 is the water velocity at the location of the pier if the pier were not there, g is the acceleration due to gravity, and B' is the projected width of the pier. The critical pier Froude Number $Fr_{c(\text{pier})}$ is given by:

$$Fr_{c(\text{pier})} = \frac{V_c}{\sqrt{g \cdot B'}} \tag{23.13}$$

where V_c is the critical velocity for the soil.

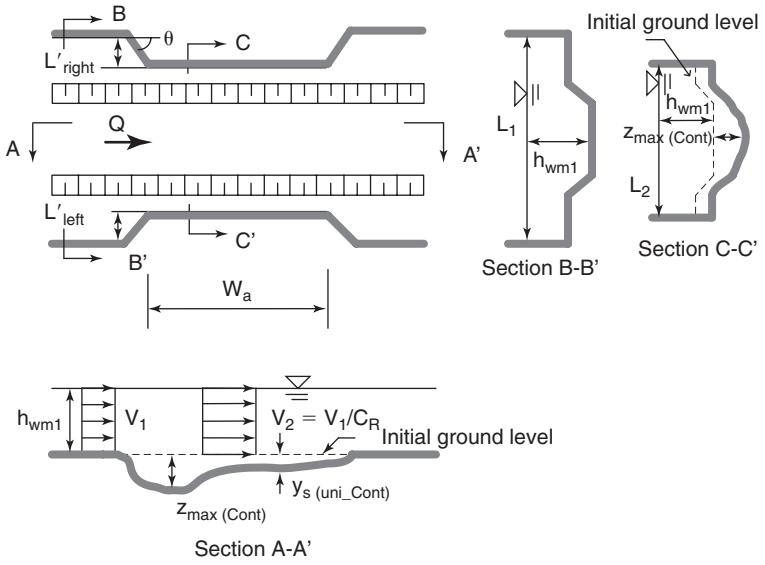

Figure 23.21 Definition of contraction scour parameters.

Contraction Scour

Contraction scour involves two regions of the river: the approach zone, called zone 1; and the contracted zone, called zone 2 (Figure 23.21).

The following equation gives the maximum scour depth for contraction scour, that is to say the maximum depth of scour that can develop in the contracted channel at the bridge location for a given set of parameters (Briaud 2012; Figure 23.21).

$$\frac{z_{\max(\text{Cont})}}{h_{wm1}} = 1.27(1.83Fr_{m2} - Fr_{mc}) \tag{23.14}$$

where $z_{\max(\text{cont})}$ is the maximum depth of contraction scour, h_{wm1} is the water depth in the main channel at the approach section, Fr_{m2} is the Froude Number for the main channel at the bridge in the contracted zone, and Fr_{mc} is the critical Froude Number for the main channel at the bridge. The Froude Number Fr_{m2} is given by:

$$Fr_{m2} = \frac{V_1/C_R}{\sqrt{gh_{wm1}}} \tag{23.15}$$

where V_1 is the velocity in the approach section, g is the acceleration due to gravity, h_{wm1} is the water depth in the main channel at the approach section, and C_R is the contraction ratio, defined as:

$$C_R = \frac{Q - Q_{block}}{Q} \tag{23.16}$$

where Q is the total discharge, and Q_{block} is the part of the discharge Q blocked by the approach embankments. The critical Froude Number Fr_{mc} is given by:

$$Fr_{mc} = \frac{V_{mc}}{\sqrt{gh_{wm1}}} = \frac{(\tau_c/\rho)^{0.5}}{gnh_{wm1}^{0.33}} \tag{23.17}$$

where V_{mc} is the critical velocity for the soil in the main channel, g is the acceleration due to gravity, h_{wm1} is the water depth in the main channel at the approach section, τ_c is the critical shear stress for the soil in the main channel, ρ is the mass density of the soil, g is the acceleration due to gravity, and n is the Manning's coefficient. Manning's coefficient characterizes the roughness of the river bottom. Estimated values are given in Table 23.4.

Table 23.4 Manning Coefficient n in $V = \frac{1}{n}R_h^{0.67}S_e^{0.5}$ *

Roughness	n ($s.m^{-0.33}$)	Roughness	n ($s.m^{-0.33}$)
Smooth clay surface	0.011	Gravel (D50 = 2 to 64 mm)	0.028 to 0.035
Sand (D50 = 0.2 mm)	0.012	Cobbles (D50 = 64 to 230 mm)	0.030 to 0.050
Sand (D50 = 0.4 mm)	0.020	Boulder (D50 > 230 mm)	0.040 to 0.070
Sand (D50 = 1 mm)	0.026		

*With V velocity in m/s, R_h hydraulic radius of channel in m, and S_e slope of the energy line (m/m).

Abutment Scour

The following equation gives the maximum scour depth for abutment scour, that is to say the maximum depth of scour that can develop around an abutment in the contracted channel at the bridge location for a given set of parameters (Briaud 2012; Figure 23.18):

$$\frac{z_{\max(Abut)}}{h_{wf1}} = 243 \times K_{ash}K_{ask}K_{al}K_{ag}\mathrm{Re}_{f2}^{-0.28} \times (1.65Fr_{f2} - Fr_{fc}) \quad (23.18)$$

where $z_{\max(abut)}$ is the maximum depth of abutment scour, h_{wf1} is the water depth in the flood plain in the approach flow next to the abutment, K_{ash} is the shape factor for abutment scour, K_{ask} is the skew angle influence factor for abutment scour, K_{al} is the influence factor taking into account the proximity of the abutment from the main channel, K_{ag} is the geometry of the channel influence factor for abutment scour, Re_{f2} is Reynolds Number around the toe of the abutment, Fr_{f2} is the Froude Number around the toe of the abutment, and Fr_{fc} is the critical Froude Number for the soil near the toe of the abutment.

The shape factor K_{ash} corrects for the fact that the parenthetical expression on the right-hand side of Eq. 23.18 was developed for a wing-wall abutment (Figure 23.22). The values of K_{ash} are:

$$K_{ash} = \begin{cases} 1.0 & \text{for wing-wall abutment} \\ 1.22 & \text{for vertical-wall abutment} \\ 0.73 & \text{for spill-through abutment with } 2:1 \text{ Slope} \\ 0.59 & \text{for spill-through abutment with } 3:1 \text{ Slope} \end{cases} \quad (23.19)$$

The skew angle factor K_{ask} corrects for the fact that the parenthetical expression on the right-hand side of Eq. 23.18 was developed for an approach embankment perpendicular to the river bank (Figure 23.23). If the embankment alignment is oblique to the river bank, the abutment scour depth is different. The equation for K_{ask} is:

$$K_{ask} = \begin{cases} 1.0 - 0.005\left(\left|\theta - 90^{\circ}\right|\right) & \text{for } 60^{\circ} \le \theta \le 120^{\circ} \\ 0.85 & \text{for other } \theta \text{ values} \end{cases} \quad (23.20)$$

where θ is the skew angle as shown in Figure 23.23.

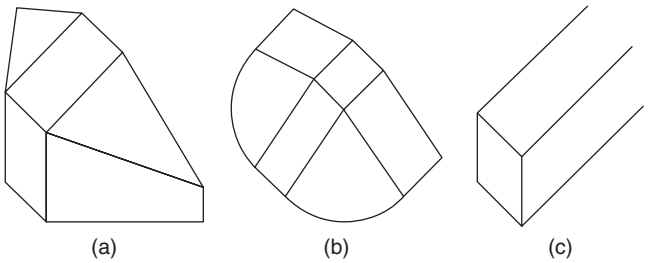

Figure 23.22 Abutment shapes: *(a)* Wing-wall abutment. *(b)* Spill-through abutment. *(c)* Vertical wall abutment.

The influence factor for the proximity of the abutment to the main channel K_{al} corrects for the fact that the parenthetical expression on the right-hand side of Eq. 23.18 was developed for an abutment far away from the bank of the main channel. When the abutment is close to the bank of the main channel, the abutment scour depth becomes larger. The equation for K_{al} is:

$$K_{al} = \begin{cases} -0.23\frac{(L_f - L_e)}{h_{wf1}} + 1.35 & \text{for } \dfrac{(L_f - L_e)}{h_{wf1}} < 1.5 \\ 1.0 & \text{otherwise} \end{cases} \quad (23.21)$$

where L_f is the length of the flood plain, L_e is the length of the embankment, and h_{wf1} is the water depth in the approach channel near the abutment.

The channel geometry influence factor K_{ag} corrects for the fact that the parenthetical expression on the right-hand side of Eq. 23.18 was developed for a compound channel geometry. For a rectangular channel geometry, the abutment scour depth is smaller. The values for K_{ag} are:

$$K_{ag} = \begin{cases} 1.0 & \text{for compound channel} \\ 0.42 & \text{for rectangular channel} \end{cases} \quad (23.22)$$

The Reynolds Number Re_{f2} is in the equation to respect the scaling laws and the influence of size. It is defined as:

$$\mathrm{Re}_{f2} = \frac{V_{f2}h_{wf1}}{\nu} \quad (23.23)$$

where h_{wf1} is the water depth in the approach channel near the abutment, ν is the kinematic viscosity of water (10^{-6} m^2/s at 20°C), and V_{f2} is the local velocity near the abutment in the flood plain, obtained as follows:

$$V_{f2} = \begin{cases} \dfrac{Q_{0.5}}{A_2}, & \text{for short setback } \left(\left(L_f - L_e\right) \le 5h_{wm1}\right) \\ \dfrac{Q_{f1}}{A_{f2}}, & \text{for long setback } (L_e \le 0.25L_f) \\ \text{otherwise use a linearly interpolated velocity between} \\ \dfrac{Q_{0.5}}{A_2} & \text{for } (L_f - L_e) = 5h_{wm1} \text{ and} \\ \dfrac{Q_{f1}}{A_{f2}} & \text{for } L_e = 0.25L_f \end{cases} \quad (23.24)$$

where $Q_{0.5}$ is the flow in half the channel defined as the sum of half the upstream flow in the main channel, 0.5 Q_{m1}, plus the flow in the flood plain immediately upstream of the abutment where the abutment is situated, Q_{f1}, h_{wm1} is the water depth in the main channel in the approach flow; A_2 is the cross sectional flow area in the contracted zone corresponding to the flow $Q_{0.5}$; A_{f2} is the cross sectional flow area on the floodplain at the contracted section; L_f is the width of the floodplain in the approach zone; and L_e is the length of embankment leading to the abutment.

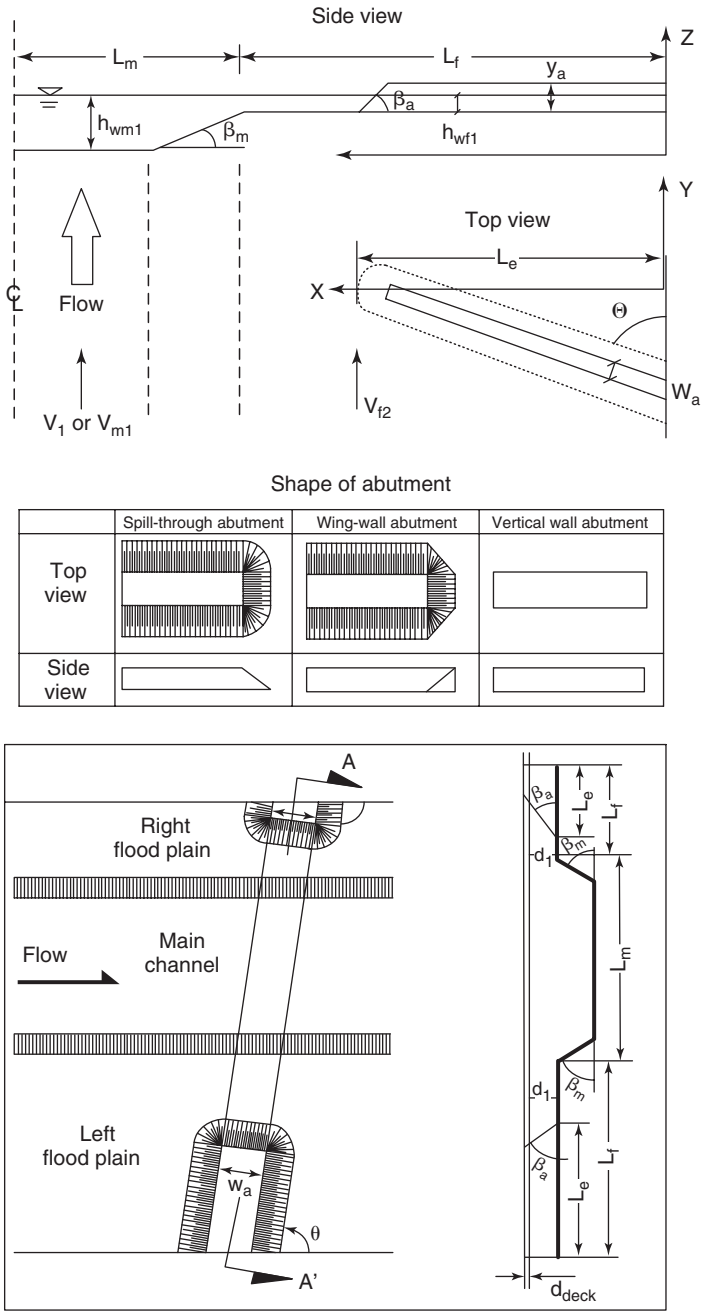

Figure 23.23 Abutment parameter definitions.

The Froude Number Fr_{f2} is calculated around the toe of the abutment and is given by:

$$Fr_{f2} = \frac{V_{f2}}{\sqrt{gh_{wf1}}} \tag{23.25}$$

where V_{f2} is defined in Eq. 23.24, g is the acceleration due to gravity, and h_{wf1} is the water depth in the approach flow near the abutment. The critical Froude Number Fr_{fc} is calculated around the toe of the abutment and is given by:

$$Fr_{fc} = \frac{V_c}{\sqrt{gh_{wf1}}} \tag{23.26}$$

where V_c is the critical velocity for the soil around the toe of the abutment, g is the acceleration due to gravity, and h_{wf1} is the water depth in the approach flow near the abutment.

23.8.2 Maximum Shear Stress at Soil–Water Boundary when Scour Begins

The maximum scour depth is the scour depth reached when the flood velocity v is applied long enough to reach $z_{\max}$. If the flood velocity stops before $z_{\max}$ is reached, then only z_{final} is reached (Figure 23.19). To predict z_{final}, it is necessary to develop the relationship between scour depth z and time t. It was found that a hyperbolic equation would fit well with

measured curves of z vs. t:

$$z = \frac{t}{\frac{1}{\dot{z}_i} + \frac{t}{z_{\max}}} \tag{23.27}$$

where z is the scour depth, $\dot{z}_i$ is the initial erosion rate at a time equal to zero under a velocity v, $z_{\max}$ is the scour depth at a time equal to infinity (asymptotic value) under a velocity v, and t is the time during which the water flows at the velocity v.

The scour depth-time curve of Eq. 23.27 is defined once $z_{\max}$ and $\dot{z}_i$ are known. The maximum scour depth $z_{\max}$ is obtained as discussed in section 23.8.1. The initial erosion rate $\dot{z}_i$ is obtained from the erosion rate vs. shear stress curve measured in the EFA test or deduced from the soil classification and Figure 23.6. Therefore, it is necessary to know the maximum shear stress $\tau_{\max}$ created by the water when it flows around the obstacle at the beginning of the scour process. The following equations were developed based on numerical simulations to calculate the shear stress $\tau_{\max}$ for pier scour, contraction scour, and abutment scour.

Maximum Shear Stress for Pier Scour

For pier scour, the equation (Nurtjahyo 2003) is:

$$\tau_{\max(\text{Pier})} = k_{pw} k_{psh} k_{psk} k_{psp} \cdot 0.094 \rho V_1^2 \left[\frac{1}{\log \text{Re}} - \frac{1}{10} \right] \tag{23.28}$$

where $\tau_{\max(\text{pier})}$ is the maximum shear stress for pier scour, k_{pw} is the water depth influence factor for pier scour shear stress, k_{psh} is the pier shape influence factor for pier scour shear stress, k_{psk} is the skew angle or angle of attack influence factor for pier scour shear stress, k_{psp} is the pier spacing influence factor for pier scour shear stress, ρ is the mass density of water, V_1 is the mean depth velocity of the water at the location of the pier if the pier were not there (also called upstream velocity in line with the pier), and Re is the pier Reynolds Number. The water depth influence factor corrects for the fact that the expression on the right-hand side of Eq. 23.28 excluding the influence factors was developed for a pier in deep water. At very shallow water depths, the shear stress $\tau_{\max}$ increases significantly. The equation for k_{pw} is:

$$k_{pw} = 1 + 16e^{(-4h_w/B)} \tag{23.29}$$

where h_w is the water depth and B is the width of the pier.

The pier shape influence factor corrects for the fact that the expression on the right-hand side of Eq. 23.28 excluding the influence factors was developed for a circular pier. For square piers, the factor is 1.15; for rectangular piers, it depends on L/B where L is the pier length and B is the pier width. The equation for k_{psh} is:

$$k_{psh} = 1.15 + 7e^{(-4L/B)} \tag{23.30}$$

where L is the length of the pier and B is the width of the pier.

The skew angle or angle of attack influence factor k_{psk} corrects for the fact that the expression on the right-hand side of Eq. 23.28 excluding the influence factors was developed for a cylindrical pier. For square and rectangular piers with a length L and a width B, the factor k_{psk} is given by:

$$k_{psk} = 1 + 1.5\left(\frac{\theta}{90}\right)^{0.57} \tag{23.31}$$

where θ is the skew angle or attack angle, which is the angle between the flow direction and the main direction of the pier (Figure 23.20).

The pier spacing influence factor k_{psp} corrects for the fact that the expression on the right-hand side of Eq. 23.28 excluding the influence factors was developed for an isolated pier. For a line of piers, the pier spacing influence factor k_{psp} is given by:

$$k_{psp} = 1 + 5e^{(-1.1S/B)} \tag{23.32}$$

where S is the center-to-center spacing of the piers and B is the width of the pier (Figure 23.20).

Maximum Shear Stress for Contraction Scour

For contraction scour, the equation for $\tau_{\max(\text{Cont})}$ (Nurtjahyo 2003) is:

$$\tau_{\max(\text{Cont})} = k_{cr} k_{cl} k_{c\theta} k_{cw} \rho g n^2 {V_1}^2 {R_h}^{-\frac{1}{3}} \tag{23.33}$$

where $\tau_{\max(\text{Cont})}$ is the maximum shear stress for contraction scour shear stress, k_{cr} is the contraction ratio influence factor for contraction scour shear stress, k_{cl} is the contraction length influence factor for contraction scour shear stress, $k_{c\theta}$ is the transition angle influence factor for contraction scour shear stress, k_{cw} is the water depth influence factor for contraction scour shear stress, ρ is the mass density of water, g is the acceleration due to gravity, n is Manning's coefficient, V_1 is the mean depth velocity of the water in the approach zone, and R_h is the hydraulic radius of the contracted channel.

The contraction ratio influence factor k_{cr} corrects for the fact that the velocity V_1 in the equation is the approach velocity, not the velocity in the contracted zone. It is given by:

$$k_{cr} = 0.62 + 0.38\left(\frac{A_1}{A_2}\right)^{1.75} \tag{23.34}$$

where A_1 is the cross-sectional flow area in the approach zone and A_2 is the cross-sectional flow area in the contracted zone.

Because A_2 is smaller than A_1, k_{cr} increases the shear stress in the contracted zone. The contraction length influence factor k_{cl} corrects for the fact that the main part of Eq. 23.33 (right hand side without correction factors) was developed for abutment widths that were larger than 0.7 times the length

of the approach embankments. For abutments narrower than that, the k_{cl} factor is given by:

$$k_{cl} = \begin{cases} 0.77 + 1.36\left(\frac{W_a}{L_1 - L_2}\right) - 1.98\left(\frac{W_a}{L_1 - L_2}\right)^2, \\ \qquad \text{for } \frac{W_a}{L_1 - L_2} \le 0.35 \\ 1.0, \quad \text{otherwise} \end{cases} \tag{23.35}$$

where W_a is the width of the top of the abutment (Figure 23.23), L_1 is the width of the river in the approach zone, and L_2 is the width of the river in the contracted zone (Figure 23.21).

The transition angle influence factor $k_{c\theta}$ corrects for the fact that the main part of Eq. 23.33 (right hand side without correction factors) corresponds to no abutment ($\theta = 0$). If the abutment appears through a nonzero transition angle, then $k_{c\theta}$ must be used; it is given by:

$$k_{c\theta} = 1.0 + 0.9\left(\frac{\theta}{90}\right)^{1.5} \tag{23.36}$$

where θ is the transition angle (Figure 23.21).

The water depth influence factor for contraction scour shear stress k_{cw} was found to be equal to 1 in all conditions.

Maximum Shear Stress for Abutment Scour

For abutment scour, the equation for $\tau_{\max(\text{Abut})}$ is:

$$\tau_{\max(Abut)} = 12.5 k_{acr} k_{aar} k_{aw} k_{ash} k_{ask} k_{al} \rho V_1^2 \text{Re}^{-0.45} \tag{23.37}$$

where $\tau_{\max(\text{Abut})}$ is the maximum shear stress for abutment scour shear stress, k_{acr} is the contraction ratio influence factor for abutment scour shear stress, k_{ash} is the influence factor for the aspect ratio of the approach embankment for abutment scour shear stress, k_{aw} is the influence factor for Froude Number for abutment scour shear stress, k_{as} is the influence factor for abutment shape for abutment scour shear stress, k_{ask} is the influence factor for the skew angle of the abutment for abutment scour shear stress, k_{al} is the influence factor related to the location of the abutment in the flood plain for abutment scour shear stress, ρ is the mass density of water, V_1 is the mean depth velocity of the water in the approach zone, and Re is the abutment Reynolds Number.

The contraction ratio influence factor k_{acr} corrects for the fact that the velocity V_1 in the equation is the approach velocity and not the local velocity around the abutment. It is given by:

$$k_{acr} = 3.65\left(\frac{Q_{tot}}{Q_{tot} - Q_{block}}\right) - 2.91 \tag{23.38}$$

where Q_{tot} is the total discharge and Q_{block} is the part of the total discharge blocked by the approach embankments.

The influence factor k_{aar} takes into account the aspect ratio of the abutment. It is given by:

$$k_{aar} = 0.85\left(\frac{L_e}{W_a}\right)^{-0.24} \tag{23.39}$$

where L_e is the length of the approach embankment and W_a is the width of the top of the abutment (Figure 23.23).

The influence factor k_{aw} takes into account the water depth. It is given by:

$$k_{aw} = \begin{cases} 2.07Fr + 0.8 \quad for \quad Fr > 0.1 \\ 1 \quad for \quad Fr \le 0.1 \end{cases} \tag{23.40}$$

where Fr is the Froude Number, defined as:

$$Fr = \frac{V_{f2}}{\sqrt{g h_{wf1}}} \tag{23.41}$$

where V_{f2} is the water velocity in the approach zone in line with the abutment and h_{wf1} is the water depth in the approach zone in line with the abutment (Figure 23.23).

The influence factor k_{ash} takes into account the shape of the abutment. It is given by:

$$k_{ash} = \begin{cases} 1.0 \quad \textit{vertical-wall abutment} \\ 0.65 \quad \textit{wing-wall abutment} \\ 0.58 \quad \textit{spill-through abutment} \end{cases} \tag{23.42}$$

The influence factor k_{ask} takes into account the skew angle of the abutment. The reference case is the case when the embankment is perpendicular to the river bank with a skew angle equal to 90°. The skew angle can be smaller or larger than 90°, but was found to have little influence on the maximum bed shear stress and is conservatively taken as equal to 1:

$$k_{ask} = 1 \tag{23.43}$$

The influence factor k_{al} takes into account the location of the abutment in the flood plain. The factor k_{al} is different from 1 only when the abutment is near the edge of the main channel. It is given by:

$$k_{al} = \begin{cases} 1.0 & for \ \left(L_f - L_e\right)/h_{wf1} \le -2 \\ 1.2 + 0.1 & for \ -2 \le (L_f - L_e)/h_{wf1} \le 0 \\ \ (L_f - L_e)/h_{wf1} & \\ 1.2 - 0.2 & for \ 0 \le (L_f - L_e)/h_{wf1} \le 1 \\ \ (L_f - L_e)/h_{wf1} & \\ 1.0 & for \ (L_f - L_e)/h_{wf1} \ge 1 \end{cases} \tag{23.44}$$

23.8.3 Final Scour Depth (z_{final}) Analysis for Constant Velocity Flow and Uniform Soil

Once the maximum shear stress $\tau_{\max}$ is known, the erosion curve linking the erosion rate $\dot{z}$ to the shear stress τ is used to find the erosion rate $\dot{z}_i$ corresponding to $\tau_{\max}$. Equation 23.27 can then be used to find out what z_{final} is, as both $z_{\max}$ and $\dot{z}_i$ are known. The following example illustrates these calculations.

A round-nose pier, with a width of 2 m and a length of 6 m, is located in a river where the water depth is 7.89 m, the approach flow velocity is 1.4 m/s, and the attack angle is 0°

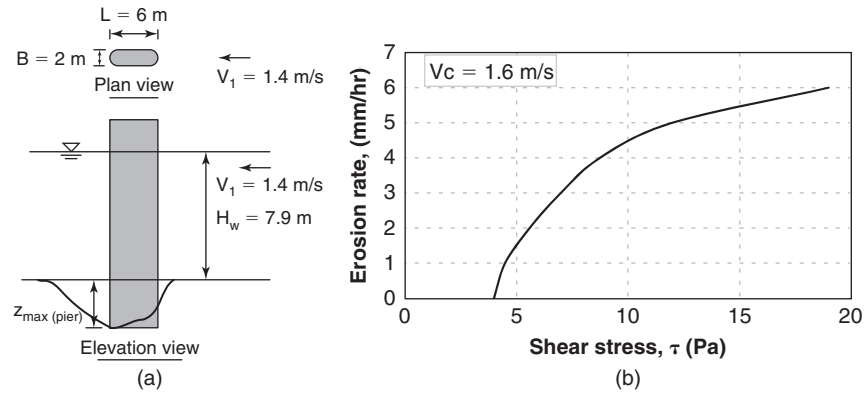

Figure 23.24 Data for example of bridge scour calculations: *(a)* Bridge pier geometry. *(b)* Erosion function of the soil.

(Figure 23.24). EFA tests were conducted on soil samples in the vicinity of the pier, and gave the average erosion function shown in Figure 23.24. The critical velocity of the soil V_c is 1.57 m/s and the duration of the flood is 48 hours. Find the pier scour depth after 48 hours of flood.

1. The maximum scour depth $z_{\max}$ is calculated first. The correction factors for water depth K_{pw}, pier shape K_{psh}, pier aspect ratio K_{pa}, and pier spacing K_{psp} are all equal to 1.0. The pier Froude Number needed in Eq. 23.8 is:

$$Fr_{(\text{pier})} = \frac{V_1}{\sqrt{g \cdot B'}} = \frac{1.4}{\sqrt{9.81 \times 2}} = 0.316 \quad (23.45)$$

and the critical pier Froude Number is:

$$Fr_{c(\text{pier})} = \frac{V_c}{\sqrt{g \cdot a}} = \frac{1.58}{\sqrt{9.81 \times 2}} = 0.356 \quad (23.46)$$

Therefore, the maximum pier scour depth $z_{\max(\text{pier})}$ is:

$$z_{\max(\text{Pier})} = 2.2 \times 1.0 \times 1.0 \times 1.0 \times 1.0 \times 2.0 \times (2.6 \times 0.316 - 0.356)^{0.7} = 2.58\,\text{m} \quad (23.47)$$

2. The maximum shear stress $\tau_{\max}$ around the pier at the beginning of the scour process is calculated next. The correction factor for water depth k_{pw} is 1.0, for pier spacing k_{psp} is 1.0, for attack angle k_{pa} is 1.0, and for pier shape k_{psh} is 1.15 ($k_{psh} = 1.15 + 7e^{-4L/B} = 1.15 + 7e^{-12}$). The pier Reynolds Number Re is 2.8×10^6 $\left(\text{Re} = \dfrac{1.4 \times 2}{10^{-6}}\right)$. Therefore, the maximum shear stress around the pier is:

$$\tau_{\max(\text{pier})} = 1.0 \times 1.15 \times 1.0 \times 1.0 \times 0.094 \times 1000 \times 1.4^2 \left(\frac{1}{\log 2800000} - \frac{1}{10}\right) = 11.7\,\text{Pa} \quad (23.48)$$

3. The initial rate of scour $\dot{z}_i$ around the pier is read on the EFA curve (Figure 23.24) at $\tau = \tau_{\max} = 11.7$ Pa, and gives 4.8 mm/hr.
4. The final depth of pier scour after 48 hours of flow can then be obtained from Eq. 23.27 as:

$$z_{final}(48h) = \frac{48}{\dfrac{1}{4.8} + \dfrac{48}{2580}} = 211\,\text{mm} \quad (23.49)$$

Therefore, the pier scour depth generated by the 48-hour flood is 8.2% of the maximum pier scour depth. Note that the erosion function used for this example corresponds to a soil with a medium resistance to erosion (Category 3) and that the flood is a relatively small flood (1.4 m/s). Major floods in rivers can reach 3 and 4 m/s. In very steep mountain torrents and at the bottom of levees during overtopping, the velocity can reach more than 10 m/s.

23.8.4 Final Scour Depth (z_{final}) Analysis for a Velocity Hydrograph and Layered Soil

Section 23.8.3 dealt with a uniform soil subjected to a constant velocity. However, in reality the flow velocity is not constant in a river, and the soil is likely to exhibit different layers versus depth. Let's look first at the velocity varying over time. The graph presenting the velocity as a function of time over many years is called a *velocity hydrograph* (Figure 23.17). This hydrograph represents an accumulation of events where the velocity v_i can be considered constant for a short period of time Δt_i. The solution (Briaud et al. 2001b) progresses by stepping into time with a time increment equal to δt_i for each iteration. For Δt_1, the velocity is V_1 and $z_{\text{final 1}}$ can be calculated. When the second velocity V_2 appears, the question is to know how to accumulate the second scour depth to the first one. The accumulation principle is as follows (Figure 23.25). The two scour depth z vs. time t curves for the velocities V_1 and V_2 are drawn separately. The scour depth $z_{\text{final 1}}$ is found on the V_2 curve and corresponds to the starting point for the scour depth increment for the second velocity.

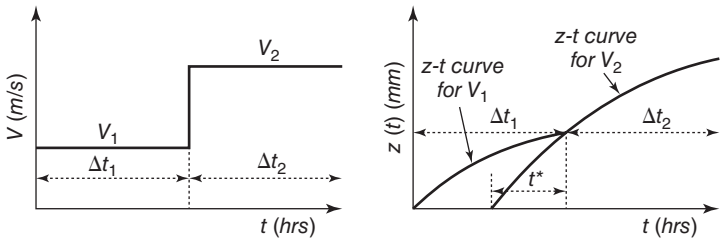

(a) Sequence of two velocities (b) Accumulation principle

Figure 23.25 Accumulation of scour depth for two consecutive floods.

The time t^* is the time required for velocity V_2 to create $z_{\text{final 1}}$. Then the scour depth due to V_2 applied for δt_2 can be calculated by using the z vs. t curve for the velocity V_2 starting at t^*. More generally, the time t^* is the time required for velocity V_i to create the same scour depth as all the previous velocities. If that scour depth is larger than $z_{\max}$ for V_i, the velocity V_i does not increase the scour depth. This accumulation principle is applied for the entire hydrograph by stepping into time over the design life of the bridge.

For a layered soil system, the process is very similar (Figure 23.26). If the soil layer 1 is H_1 thick, the scour depth is predicted as a function of time by using the erosion function of soil 1 and the velocity accumulation principle. When the scour depth becomes equal to H_1, the erosion function is switched to that of soil layer 2 and the time t^* required for the first velocity impacting soil layer 2 to generate a scour depth equal to H_1 is found. After that, the calculations proceed using the erosion function of layer 2. These two algorithms have been automated in a program called SRICOS-EFA and are available at http://ceprofs.tamu.edu/briaud/.

The SRICOS-EFA method also allows the user to develop a probability of exceedance P vs. scour depth z curve so that the engineer can choose a scour depth corresponding to an acceptable probability of exceedance. The steps to develop the P-z curve are as follows (Brandimarte et al. 2006; Briaud et al. 2007a; Bolduc et al. 2008). First, the flow values in the hydrograph for the chosen period of time are organized in a log normal cumulative distribution function. Second, a random number generator is used to sample that distribution and create, say, 1000 equally likely future hydrographs. Third, for each of these 1000 future hydrographs, the final depth of scour, Z_{final}, is obtained according to the SRICOS-EFA method. Fourth, the 1000 values of Z_{final} are organized in a log normal distribution and presented as a cumulative density function referred to earlier as the P-z curve. This process is an integral part of the SRICOS-EFA computer program (Kwak et al. 2001; http://ceprofs.tamu.edu/briaud/).

The following case history gives an example of the calculation of scour depth, including probabilistic results.

23.8.5 The Woodrow Wilson Bridge Case History

The following case history (Kwak et al. 2002) describes the process followed to evaluate the scour depth around the main piers of the Old Woodrow Wilson Bridge, which carried I-95 across the Potomac River in Washington, D.C., from 1960 when it was built until 2005 when it was replaced.

Soil Erodibility

The soil stratigraphy is presented in Figure 23.27. It shows that at the location of the main pier in the main channel, the soil stratigraphy consists of a soft organic clay overlying a layer of hard plastic clay. Twelve ASTM Standard thin-wall steel tube samples were collected at the bottom of the Potomac River and sent to Texas A&M University for EFA testing. Examples of the erosion functions obtained for samples close to the main pier are shown in Figure 23.28. As can be seen, the soft layer has a much higher critical velocity than the hard

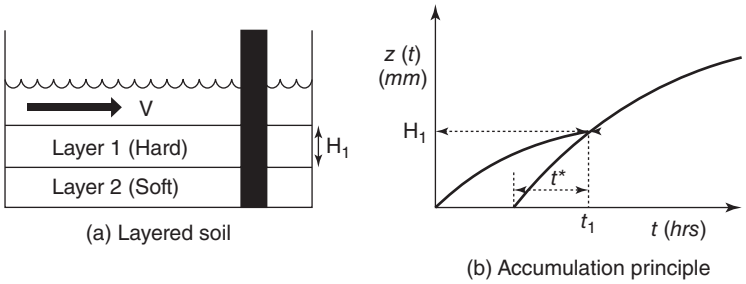

(a) Layered soil (b) Accumulation principle

Figure 23.26 Scour depth for a layered soil system.

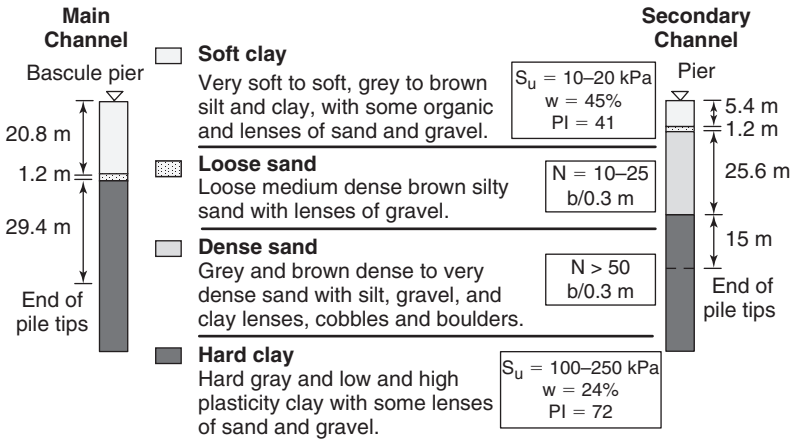

Figure 23.27 Soil stratigraphy at the location of the New Woodrow Wilson Bridge.

clay below, demonstrating yet again that critical velocity does not necessarily increase with shear strength.

Water Velocity

The nearest gage station (Gage Station 01646500; www.usgs.gov) on the Potomac River is located approximately 13 km upstream of the Woodrow Wilson Bridge and has a drainage area of 29,965 km^2. The discharge hydrograph from this gage station was multiplied by the drainage area ratio between the bridge location and the gage location (30742/29965) to obtain the discharge hydrograph at the bridge (Figure 23.29). The program HEC-RAS (Hydrologic Engineering Center's River Analysis System) (Brunner 2002) is a commonly used 1D flow analysis program. It was used to develop the relationship between the discharge and the velocity on the one hand and the relationship between the discharge and the water depth on the other (Figure 23.30). Note that the velocity in Figure 23.30 is the mean depth velocity of the water at the main pier location if the bridge were not there. That is the velocity, also called *approach velocity*, used in pier scour depth calculations. Using these relationships, the discharge vs. time curve was transformed into the water depth hydrograph and into the velocity hydrograph or velocity vs. time curve (Figure 23.31).

Geometry of the Obstacle

The old Woodrow Wilson Bridge was a bascule bridge and the obstacle to the flow considered for this case history was the main bascule pier for the bridge. The pier is square and 9.75 m by 9.75 m in plan view. The attack angle is zero, as the pier is in line with the flow.

Scour Depth Calculations

The time step for the 38-year period of observation (1960 to 1998) was chosen as one day, for a total of 13,870 time steps. The scour depth calculations progressed one day at

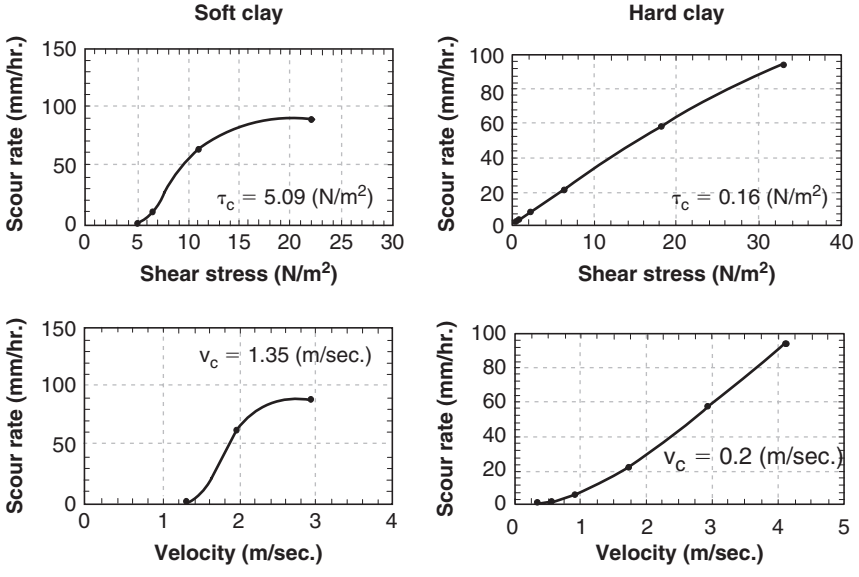

Figure 23.28 Erosion functions for the two main soil layers at the main pier location.

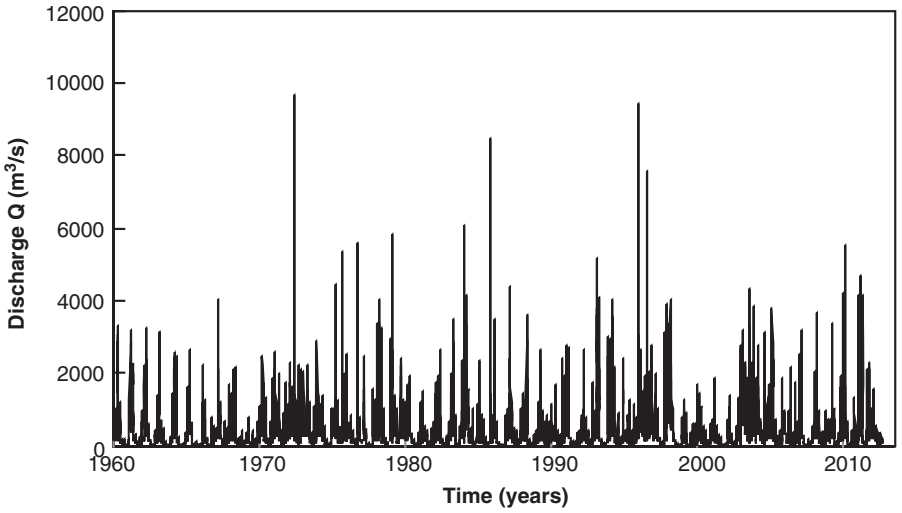

Figure 23.29 Discharge hydrograph (1960-2012) for the Potomac River at the Woodrow Wilson Bridge.

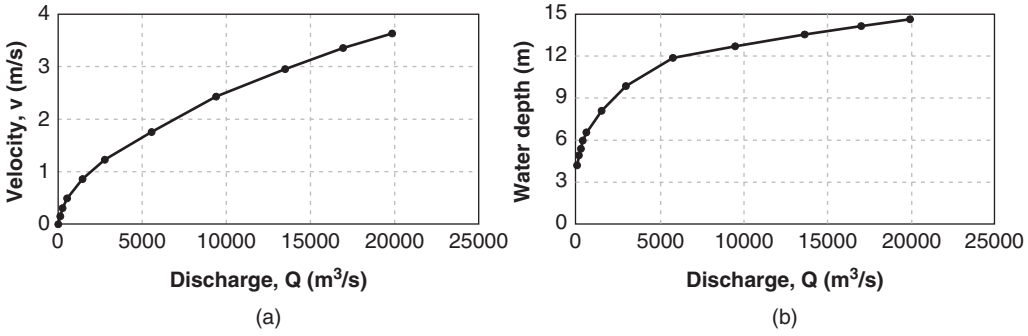

Figure 23.30 Calculated relationship between discharge, velocity, and water depth at the Woodrow Wilson Bridge if the bridge were not there.

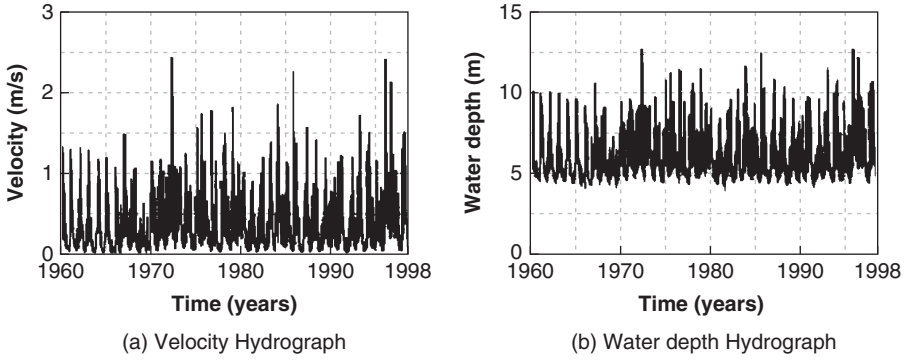

Figure 23.31 Velocity and water depth hydrograph.

a time by following the accumulation principle detailed in section 23.8.4. The program SRICOS-EFA (https://ceprofs.civil.tamu.edu/briaud/) was used with the soil erosion functions, the water velocity and water depth hydrographs, and the pier geometry as input. The resulting scour depth vs. time plot is shown in Figure 23.32.

The same procedure was repeated to predict the scour depths at the other piers of the old Woodrow Wilson Bridge

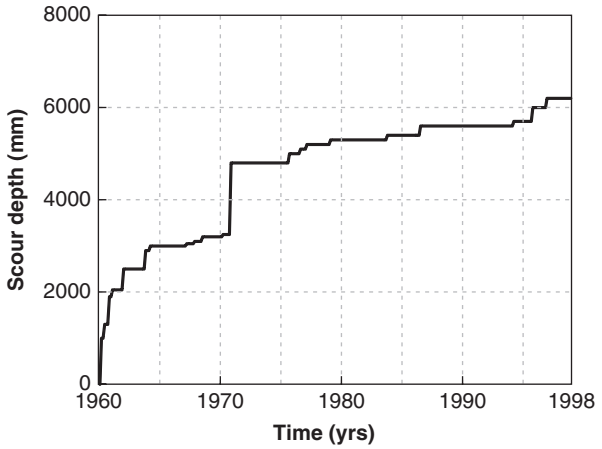

Figure 23.32 Predicted scour depth vs. time for pier 1E of the Old Woodrow Wilson Bridge.

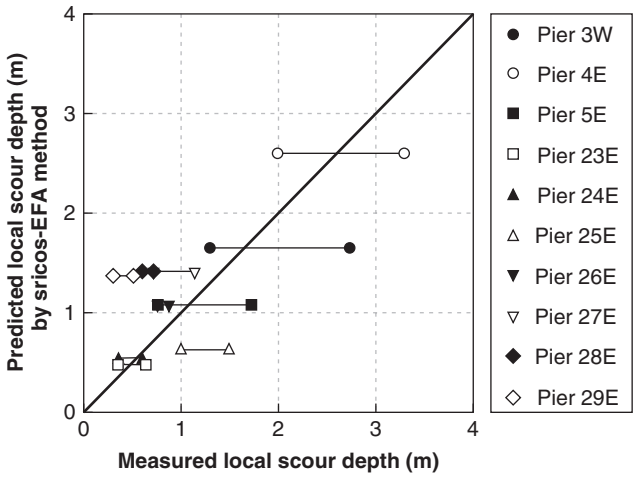

Figure 23.33 Predicted vs. measured scour depths at the old Woodrow Wilson Bridge.

where measured values were available (Hunt 2001). The comparison between predicted and measured values for all the piers that did not have rip-rap protection and where scour depth measurements were collected as a function of time is shown in Figure 23.33 (Kwak et al. 2002).

Probabilistic Scour Calculations

Figure 23.34 is an example of a probability vs. scour depth P-z curve for values of the design life L_t of the bridge. With this graph, the engineer can decide at what probability of exceedance to operate and choose the corresponding scour depth.

23.9 RIVER MEANDERING

23.9.1 Predicting River Meandering

Rivers are active system where meanders can move laterally several meters per year. This lateral migration of the main channel affects bridges, embankments, and other structures straddling the river. It is important to predict future meander movements to design remedial measures or move the structure. Many have contributed to the advancement of knowledge in this field, including Brice (1974), Hickin and Nanson (1984), Hooke (2001), Lagasse et al. (2001), and W. de Moor et al. (2007). Briaud et al. (2007a) developed the MEANDER method to predict the movement of a meander over time. It proceeds along the same steps followed to predict scour depth. First, the initial geometry of the river is described by fitting circles to the meander bends and placing straight-line tangents to the circles between circles. Second, the erosion function of the river banks is input. This can be done by using the results of EFA tests or by using the erosion classification charts of Figures 23.6 and 23.7 adjusted for the presence of vegetation, trees, or other erosion-retarding layers. Third, the velocity hydrograph is input from measurements at a nearby gage station. Fourth, the circles describing the meanders are moved according to erosion rules developed through a series of very large-scale laboratory meander experiments (in sand and then in clay) as well as numerical simulations (Briaud et al. 2007a; Wang 2006; Park 2007; Yeh

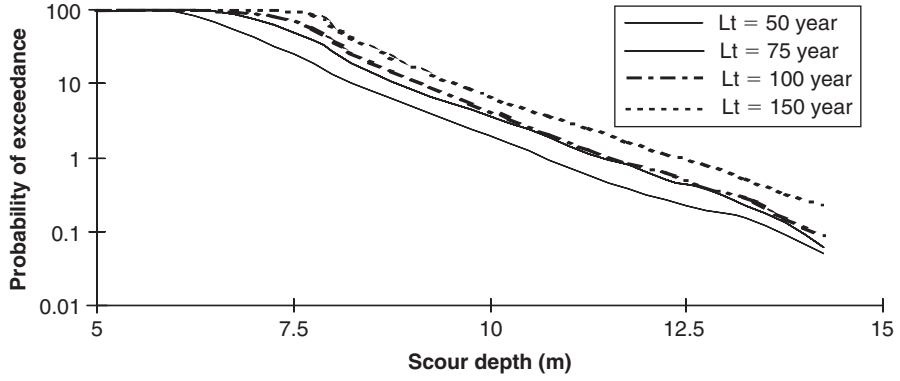

Figure 23.34 Probability of exceedance over the design life vs. scour depth curve for the bascule pier of the new Woodrow Wilson Bridge.

2008). This leads to a prediction of the location of the river after the period of time corresponding to the hydrograph.

The MEANDER method also allows the user to develop a map indicating the probability that the river will move a certain distance or more. The steps to develop that probabilistic river location are as follows (Briaud et al. 2007a). First, the flow values in the hydrograph for the chosen period of time T are organized in a log normal cumulative distribution function. Second, a random number generator is used to sample that distribution and create, say, 1000 equally likely future hydrographs. Third, for each of these 1000 future hydrographs lasting a time T, the final location of the river is obtained according to the MEANDER method. Fourth, the 1000 traces of the future river location are organized in a probabilistic map (Briaud et al. 2007b). This map gives the location of the river corresponding to the probability that the river will reach that location or go further after a time t. A conceptual example of this probabilistic map is shown in Figure 23.35 for a period of 20 years. This process is an integral part of the MEANDER computer program (http://ceprofs.tamu.edu/briaud/). The following case history illustrates the meander migration calculation process.

23.9.2 The Brazos River Meander Case History (Park 2007)

The river is the Brazos River in Texas, USA. The meander is located near Navasota, Texas (Figure 23.36) and the bridge carries highway SH105 over the Brazos River.

Observations

Records indicate that the meander has migrated significantly and rather steadily over a long period of time. Figure 23.36 shows the migration rate, which averages 4 m/yr. Observations at the site and large-scale laboratory experiments at Texas A&M University (Wang 2006; Park 2007; Yeh 2008) indicate that the process by which the meander progresses is

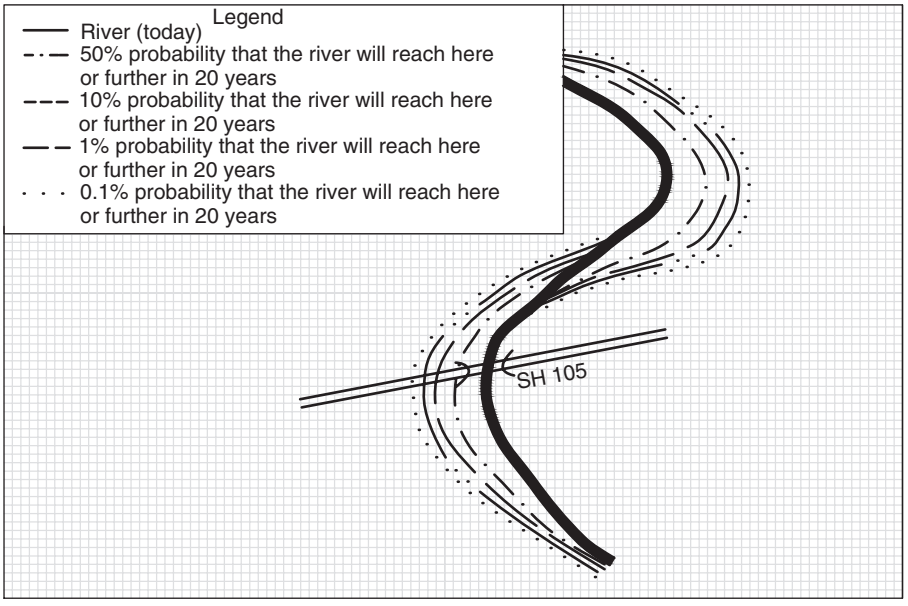

Figure 23.35 Conceptual presentation of the meandering risk for a river.

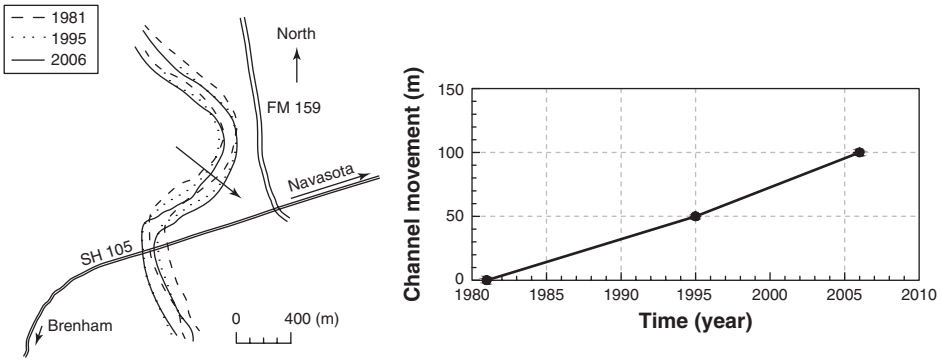

(a) River migration from 1981 to 2006 (b) Meander migration versus time

Figure 23.36 Measured migration of the meander over a 25-year period.

erosion of the base of the exterior river bank, which undercuts the steep slopes and leads to overhang failures of the banks. The material that falls into the flow is then moved to the other side of the main channel and slightly downstream. This cross-channel movement is due to the helical flow of the water in the meander. Such helical flow has been experimentally measured and numerically reproduced (Yeh 2008; Briaud et al. 2007a). This process leads to the formation of sand bars on the inside of the meander and to steep banks on the outside of the channel (Figure 23.37).

Soil Erodibility

Borings were done at the site of the meander from the top of the bank. The stratigraphy according to boring B-2 (Figure 23.38) shows 8 m of clay underlain by 7 m of sand. Thin-wall steel tube samples were collected and tested in

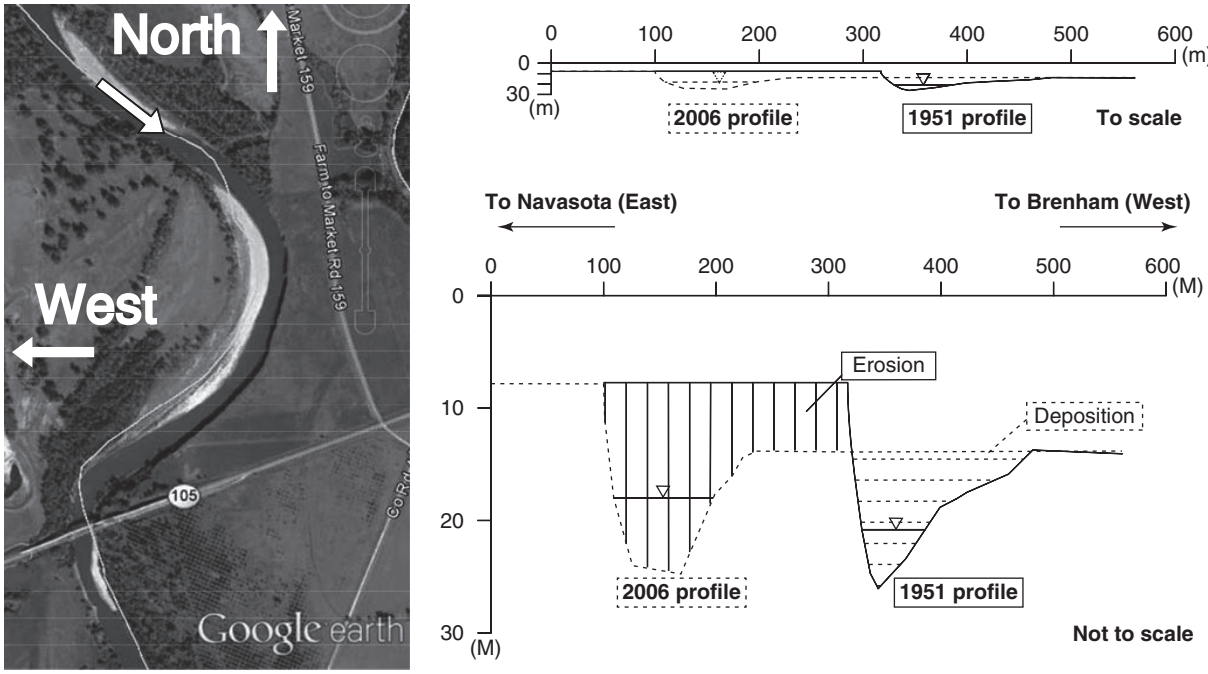

Figure 23.37 Lateral movement of the main channel between 1951 and 2006.

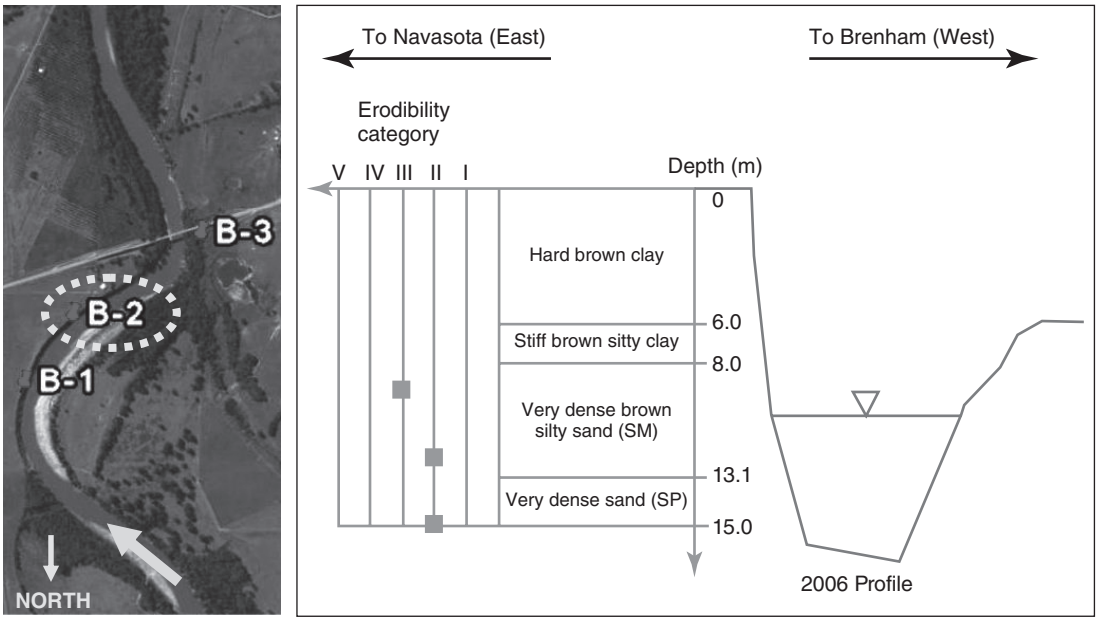

Figure 23.38 Soil stratigraphy at boring B-2.

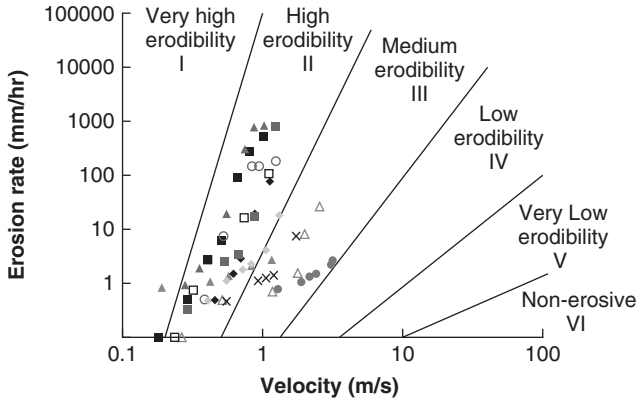

Figure 23.39 EFA test results on the soil from the meander bank.

the EFA. The results are shown in Figure 23.39. As could be predicted, the deeper layers were more erodible than the shallow ones. This means that the sand layer below will erode faster than the clay layer above. This will undercut the overhanging clay and lead to sloughing, as observed in the field. The prediction of meander migration was made using the erosion function of the deeper sand layer, as it was the controlling layer in this case.

Water Velocity

Gage Station ST #08110200 is located at the SH105 bridge over the Brazos River very close to the meander where the data were collected. This gage station worked from 1965 to 1987. To obtain the hydrograph over the prediction period 1958 to 2006, a process was developed (Park 2007) to make use of other nearby stations that had longer records (ST #08110200, ST #08108700, and ST #08109000). Then the relationship between discharge, velocity, and water depth was obtained from the actual measurements made during the period of 1965 to 1987 at gage ST #08110200. The velocity hydrograph of Figure 23.40 was finally obtained.

Geometry of the Obstacle

In this case, the obstacle is the shape of the meander, which is characterized primarily by its radius of curvature R and the width of the river channel W. To obtain R, a circle is fitted to the meander and the radius of the best-fit circle is retained as the value of R. The bend angle Φ is the angle to the center of that circle bounded by the beginning and the end of the meander on that circle. Any point M on the meander is then identified by the angle θ between the beginning and point M. Migration of the meander at point M is predicted as the movement over a period of time in the direction of the circle radius.

Meander Migration Calculations

The program MEANDER (http://ceprofs.tamu.edu/briaud/) was used to predict the migration of the meander over the period of time 1981 to 2006. The measured river centerline and the predicted river centerline are shown in Figure 23.41.

23.10 LEVEE OVERTOPPING

23.10.1 General Methodology

Levees or *dikes* are small dams built along a river or an ocean to prevent the water from inundating the land in case of flood. The top of the levee is set at a predetermined height corresponding to the water level for a chosen design flood. This flood corresponds to a certain return period, such as a 100-year flood. If the flood exceeds the design return period, water is likely to flow over the levee and generate potential erosion. One of the first observations is that if the water flows above a levee of height H, by the time the water reaches the bottom of the dry side of the levee it will have a velocity V, which can be very high. One simple way to evaluate that velocity is to write conservation of energy:

$$mgH = \frac{1}{2}mV^2 \quad or \quad V = \sqrt{2gH} \tag{23.50}$$

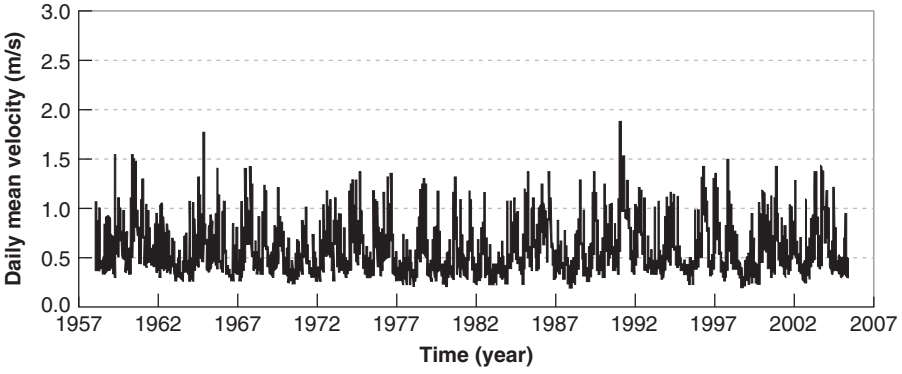

Figure 23.40 Velocity hydrograph for the Brazos River meander.

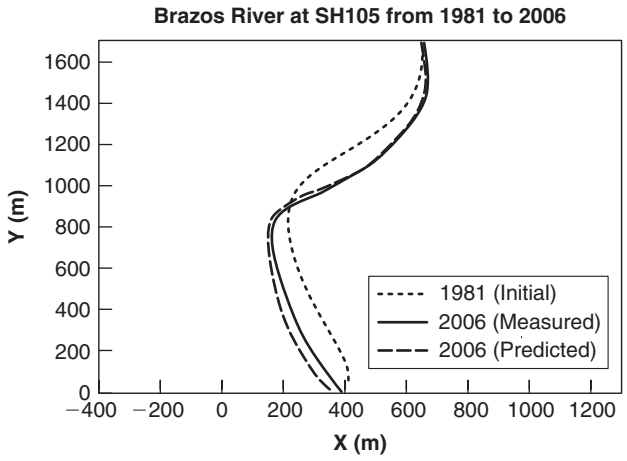

Figure 23.41 Predicted and measured migration of the Brazos River from 1981 to 2006.

For example, if the levee is 5 m high, the velocity V will be approximately 10 m/s. Of course, Eq. 23.50 does not take into account the energy lost in friction between the water and the levee surface, but it does indicate that the velocity range is much higher than typically encountered in rivers, where water rarely flows faster than 3 to 4 m/s. Furthermore, a distinction should be made between events such as hurricanes on one hand and river floods on the other. The major distinction is that hurricanes may overtop a levee for about 2 hours, whereas river floods may overtop a levee for 2 days. A levee-overtopping erosion chart developed for these two types of events is presented in Figure 23.42. It indicates which soil categories and associated erosion functions are likely to resist overtopping during a 2-hour and a 2-day overtopping. Recall that categories I to IV on the erosion chart are soils and categories V and VI are rocks. As can be seen, only the most erosion-resistant soils can resists 2 hours of overtopping without protection (Category IV), and no soil can sustain 2 days of overtopping without being totally eroded away. Armoring or vegetation satisfying strict criteria must be used to ensure that overtopping can be sustained for longer than 2 hours.

Vegetation can help significantly in retarding erosion. To be effective, though, this vegetation has to satisfy the following minimum requirements: It should have a mat-like appearance, have a sod-forming root system, be made of perennial grasses, have a dense consistent coverage, and have a minimum height of 0.3 m during flood season. Tree roots can be considered to help reinforce the levee slope, however, a the tree on a levee that is uprooted by a storm will create a major hole in the levee. Also, if the tree dies, the disappearance of the roots will leave channels for the water to seep through the levee. On the whole, trees on levees or near levees are not a good idea.

The following case history illustrates how the levee overtopping chart was generated and how it can be used.

23.10.2 Hurricane Katrina Levee Case History: New Orleans

On August 29, 2005, levee overtopping and associated erosion contributed significantly to the Katrina hurricane disaster in New Orleans, where some places are 6 m below the tops of the levees. This case history (Briaud 2006b) describes the process by which overtopped levees erode and discusses whether unprotected soils can resist overtopping erosion.

Soil Erodibility

Thin-wall steel tube samples and bag samples were obtained from the top of the levees at shallow depth (0 to 1 m). These samples were collected from locations S1 through S15 in Figure 23.43. The bag samples were reconstituted in a Shelby tube by recompacting the soil at a low and at a high compaction effort (Briaud 2006b). The soil type varied widely, from loose, uniform fine sand to high-plasticity stiff clay. EFA

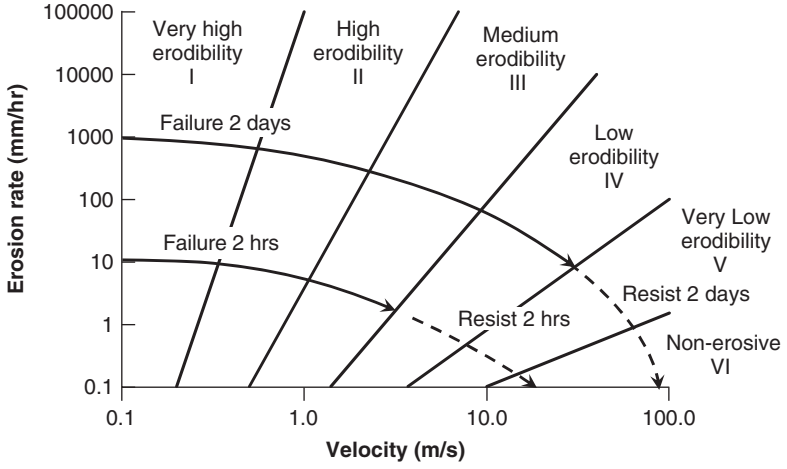

Figure 23.42 Levee overtopping.

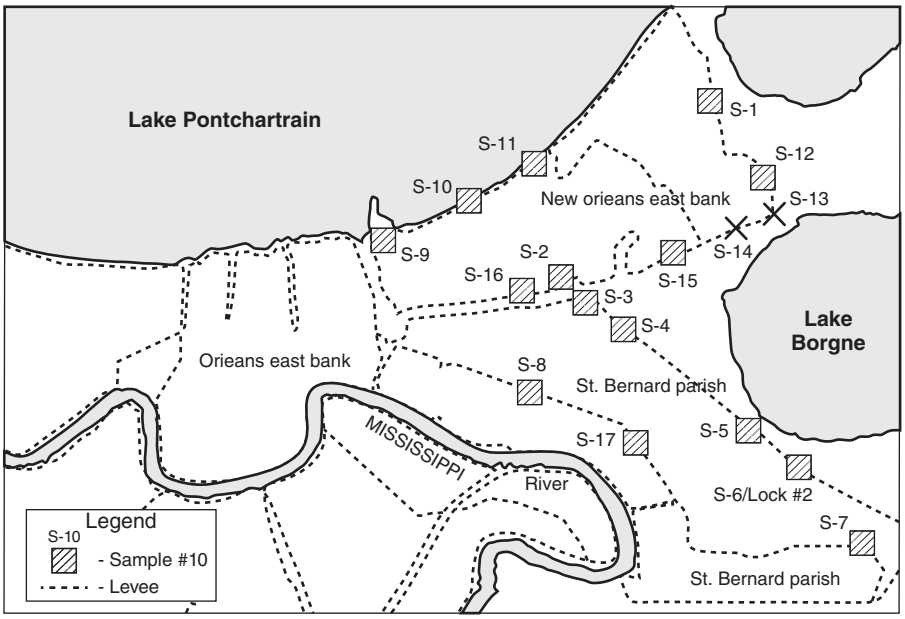

Figure 23.43 Location of shallow samples collected from the top of the levees.

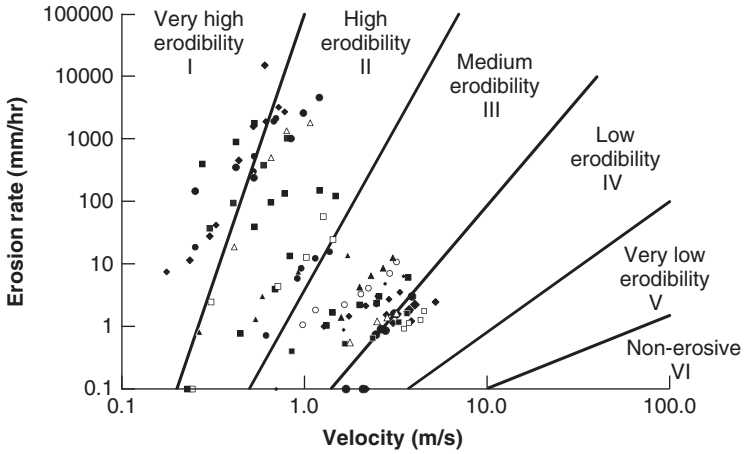

Figure 23.44 EFA test results in terms of velocity for some levee soils.

tests were performed on the samples. The results of all the tests are shown in Figures 23.44 and 23.45. One of the first observations from those figures is that the erodibility of the soils obtained from the New Orleans levees varies widely, all the way from very high erodibility (Category 1) to low erodibility (Category 4). This explains in part why some of the overtopped levees failed while other overtopped levees did not.

Water Velocity

Hurricanes are large rotating masses of moisture that can be 400 km in diameter. They travel relatively slowly at speeds of about 40 km/hr. Therefore, a hurricane takes about 10 hours to go over a levee or a bridge. The worst part of the storm, however, is only a fraction of that time. The friction generated by the wind at the air-water interface drags the water into a storm surge that can reach several meters above the mean sea level and kilometers in length. The surge associated with Katrina was about 8.5 m at Bay St. Louis, 4.6 m at Lake Borgne, and 3 m at Lake Pontchartrain. The storm surge was high enough to overtop some of the levees. As discussed earlier, the water velocity at the bottom of such levees can reach 10 m/s.

Geometry of the Obstacle

Most levees around New Orleans are between 3 and 6 m high. They have two main shapes. The first one consists of a flat top that is some 4 m wide with side slopes at about 5 horizontal to 1 vertical. Because the width of such a levee configuration takes a lot of space, the second shape consists of the same shape as the first, but at a reduced scale with a vertical wall

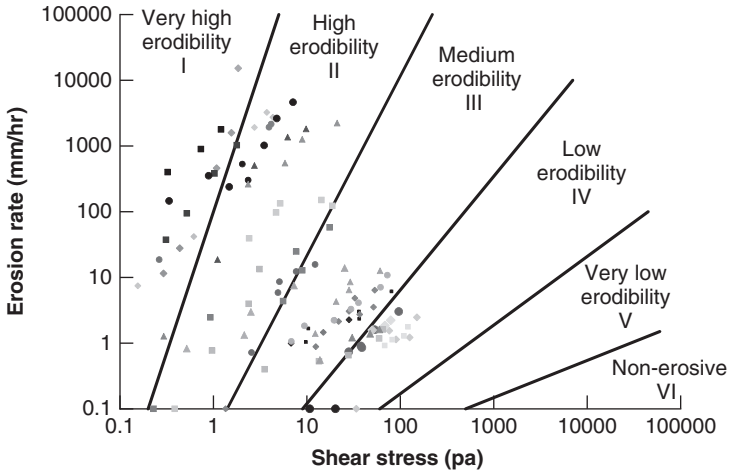

Figure 23.45 EFA test results in terms of shear stress for some levee soils.

extending from the top of the levee. The problem addressed here is limited to the first shape (no wall).

Predicting Levee-Overtopping Erosion

There was overwhelming evidence that the water overtopped the levees in many places; such evidence consisted mostly of ships being trapped on top of the levees when the water receded, but also included debris stuck in trees at levels higher than the top of the levees. Some levees resisted the overtopping well, whereas some levees were completely eroded. In Figure 23.46, the erodibility functions for the samples taken from levees that were overtopped and resisted well are plotted as open circles; the solid dots are for the samples of levees that were completely eroded. As can be seen, the eroded levees were made of soils in erodibility categories 1 and 2, whereas the levees that resisted well were made of soils in erodibility categories 3 and 4. This led to the levee overtopping chart shown in Figure 23.42.

23.11 COUNTERMEASURES FOR EROSION PROTECTION

Countermeasures for erosion protection include a number of solutions, the most prevalent of which is the use of rip rap (Figure 23.47). Rip rap can be sized by the following equation (USACE 1991):

$$d_{30} = H_w F\, C_{st} C_v C_t \left(\frac{V_{des}}{\sqrt{C_{sl}\left(G_s - 1\right) g H_w}} \right)^{2.5} \qquad (23.51)$$

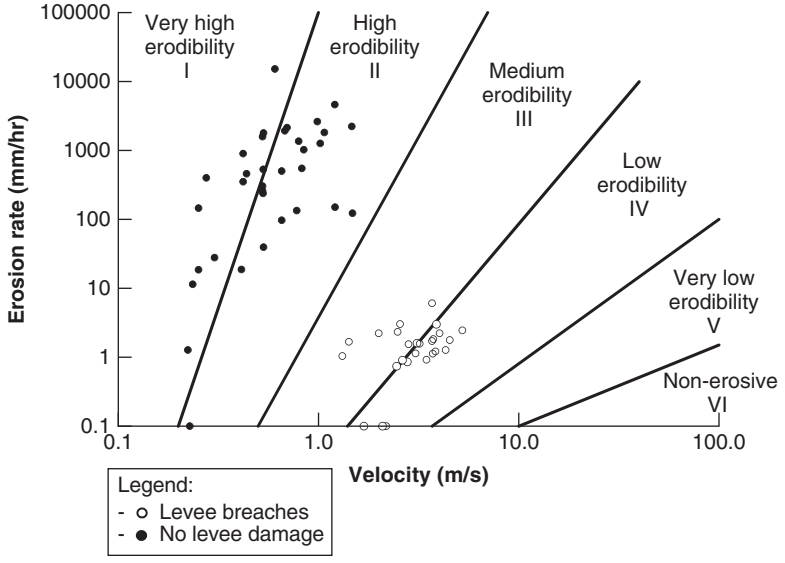

Figure 23.46 EFA test results for the soils of levees that failed and for the soils of levees that did not fail by overtopping erosion.

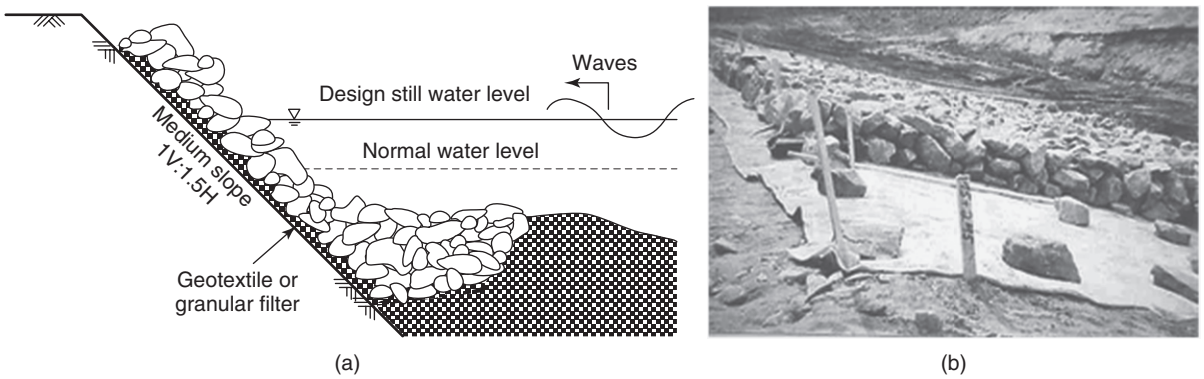

Figure 23.47 Rip rap with geosynthetic filter installation: *(a)* Design plan. *(b)* Field installation. (*Right picture*: Courtesy of FHWA.)

where d_{30} is the particle size of the rip-rap grain size distribution curve corresponding to 30% fines, H_w is the water depth, F is the factor of safety, C_{st} is the stability coefficient, C_v is the velocity distribution coefficient, C_t is the blanket thickness coefficient, V_{des} is the mean depth water velocity, C_{sl} is the side slope correction factor, G_s is the specific gravity of the rip rap, and g is the acceleration due to gravity (9.81 m/s^2).

The stability coefficient C_{st} takes into account the roughness of the rip-rap blocks; it is 0.3 for angular rock and 0.375 for round rocks. The velocity distribution coefficient C_v takes into account the fact that water tends to accelerate on the outside of river bends; it is 1 for straight channels and inside of bends, and 1.23 in most other cases. The blanket thickness coefficient C_t is a function of the rip-rap gradation, with a default value of 1 in the absence of additional data. The velocity V_{des} is the mean depth velocity for straight channels. For river bends it is given by:

$$V_{des} = V_{ave}\left(1.74 - 0.52\log\frac{R_c}{W}\right) \tag{23.52}$$

where V_{ave} is the mean depth velocity upstream of the bend, R_c is the centerline radius of curvature of the river bend, and W is the river width at the water level.

The side slope coefficient C_{sl} is given by:

$$C_{sl} = \sqrt{1 - \left(\frac{\sin(\theta - 14^\circ)}{\sin 32^\circ}\right)^{1.6}} \tag{23.53}$$

where θ is the bank angle in degrees. The specific gravity of solids G_s is usually taken as 2.65.

It is very important to place a filter between the soil to be protected and the rip-rap layer. Without a filter, the soil under the rip rap may continue to erode through the large voids in the rip rap. In the end, the rip rap may not move away, but may simply go down significantly as the underlying soil erodes away. The filter may be a sand filter or a geosynthetic filter (see Chapter 27). Design guidelines can be found in Heibaum (2004) for sand filters and in Koerner (2012) for geosynthetic filters.

Other countermeasures to prevent erosion include (Lagasse et al. 2009):

1. Flow deflectors such as spurs, jetties, dikes, and guide banks
2. Rigid armoring of the soil surface, such as soil-cement mixing and grouted mattresses
3. Flexible armoring, such as rip rap, gabions, and articulated blocks
4. Pier geometry modification, such as slender pier shape and debris deflectors
5. Vegetation such as woody mats and root wads
6. Fixed and portable instrumentation such as sonars and float-out devices
7. Periodic inspection

23.12 INTERNAL EROSION OF EARTH DAMS

23.12.1 The Phenomenon

It is estimated that 46% of earth dam failures occur due to internal erosion, and half of those failures occur during the first filling of the reservoir (Fell et al. 2005; Figure 23.48). Yet, handling of internal erosion of earth dams is still based primarily on engineering judgment and experience. Although guidelines and publications exist, much remains to be studied and researched in this field. For internal erosion of an earth dam to take place, the following are required:

1. A seepage flow path and a source of water
2. Erodible material that can be carried by the seepage flow within the flow path
3. An unprotected exit from which the eroded material may escape
4. For a pipe to form, the material must be able to form and support the roof of the pipe

Four different phenomena can lead to internal erosion of an earth dam (Figure 23.49):

1. Backward erosion
2. Concentrated leak

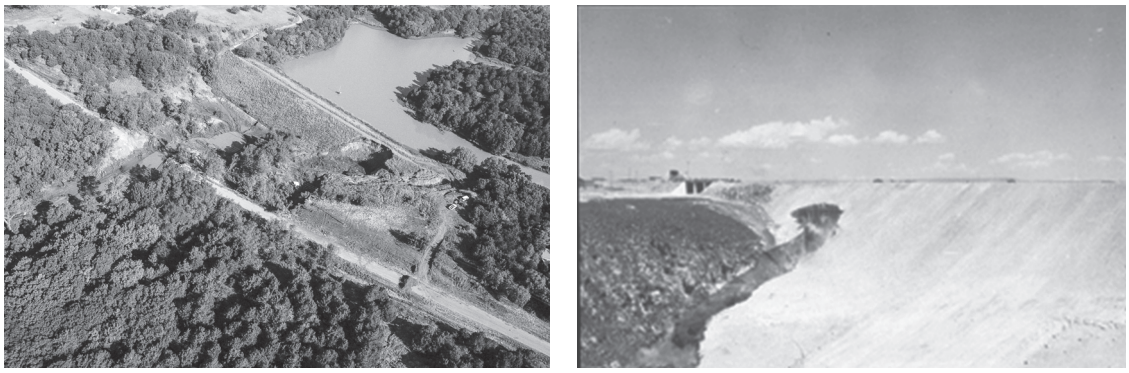

(a) (b)

Figure 23.48 Internal erosion of an earth dam. (a) Blackman Creek Dam. (b) Teton Dam. (a: Photograph by Mark S. Harrison, Oklahoma Conservation Commission. Used by permission. b: Courtesy of Eunice Olson.)

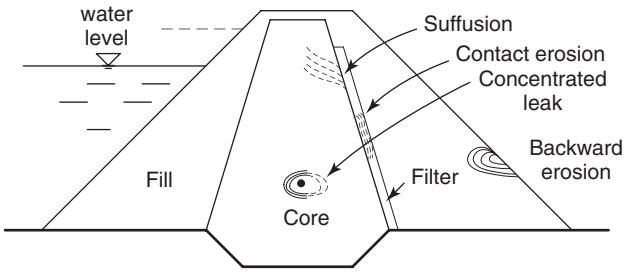

Figure 23.49 Mechanisms of internal erosion failures. (After Prezlmaier 2005)

3. Suffusion
4. Soil contact erosion

Backward erosion is initiated at the exit point of the seepage path when the hydraulic gradient is too high and the erosion gradually progresses backward, forming a pipe. A *concentrated leak* is internal to the soil mass; it initiates a crack or a soft zone emanating from the source of water and may or may not progress to an exit point. Erosion gradually continues and can create a pipe or a sinkhole. *Suffusion* develops when the fine particles of the soil wash out or erode through the voids formed by the coarser particles. This occurs when the amount of fine particles is smaller than the void space between the coarse particles. If, in contrast, the soil has a well-graded particle size distribution with sufficiently small voids, suffusion is unlikely. Soils are called internally unstable if suffusion takes place and internally stable if particles are not eroding under seepage flow. *Soil contact erosion* refers to sheet flow at interfaces between soil types. It may occur, for example, when water seeps down the back face of the core at the interface with the filter and then the stabilizing mass.

Earth dams deform during and after construction. This movement can be compression, extension, and/or shear distortion. Because typical dams are made of different zones playing different roles, they exhibit different deformation characteristics. This can lead to differential movement, resulting in cracks or soft zones where internal erosion can be initiated. Shrinkage can also create cracks that are prone to erosion if water comes to flow through them. Fell and Fry (2005) summarize the most likely locations where internal erosion can start in an earth dam (Figure 23.50).

23.12.2 Most Susceptible Soils

Coarse silt and fine sand are among the most erodible soils. Therefore, earth dams containing significant amounts of such materials will be more prone to internal erosion. Clays in general, and high-plasticity clays in particular, are more resistant to erosion as long as the electrical bonds between particles are not destroyed by chemicals. It seems that some core materials of glacial origin, such as glacial tills, can be particularly susceptible to internal erosion. Sherard (1979) gives a range of gradation of soils that can lead to internal erosion problems (Figure 23.51).

The soils that are most susceptible to suffusion are those where the volume of fines is less than the volume of the voids between coarse particles. In this case, the fines can move easily between the coarse particles and erode away to an exit face. After suffusion, such soils are devoid of fines and become very pervious clean gravel, for example. Fell and Fry (2005) indicate that gap-graded soils and coarsely graded soils with a flat tail of fines (Figure 23.52) are most susceptible to suffusion.

23.12.3 Criterion to Evaluate Internal Erosion Potential

One of the important criteria for evaluating erosion is to calculate the hydraulic gradient and compare it to the critical gradient. The critical gradient is given by:

$$i_{cr} = \frac{\gamma_{sat} - \gamma_w}{\gamma_w} \tag{23.54}$$

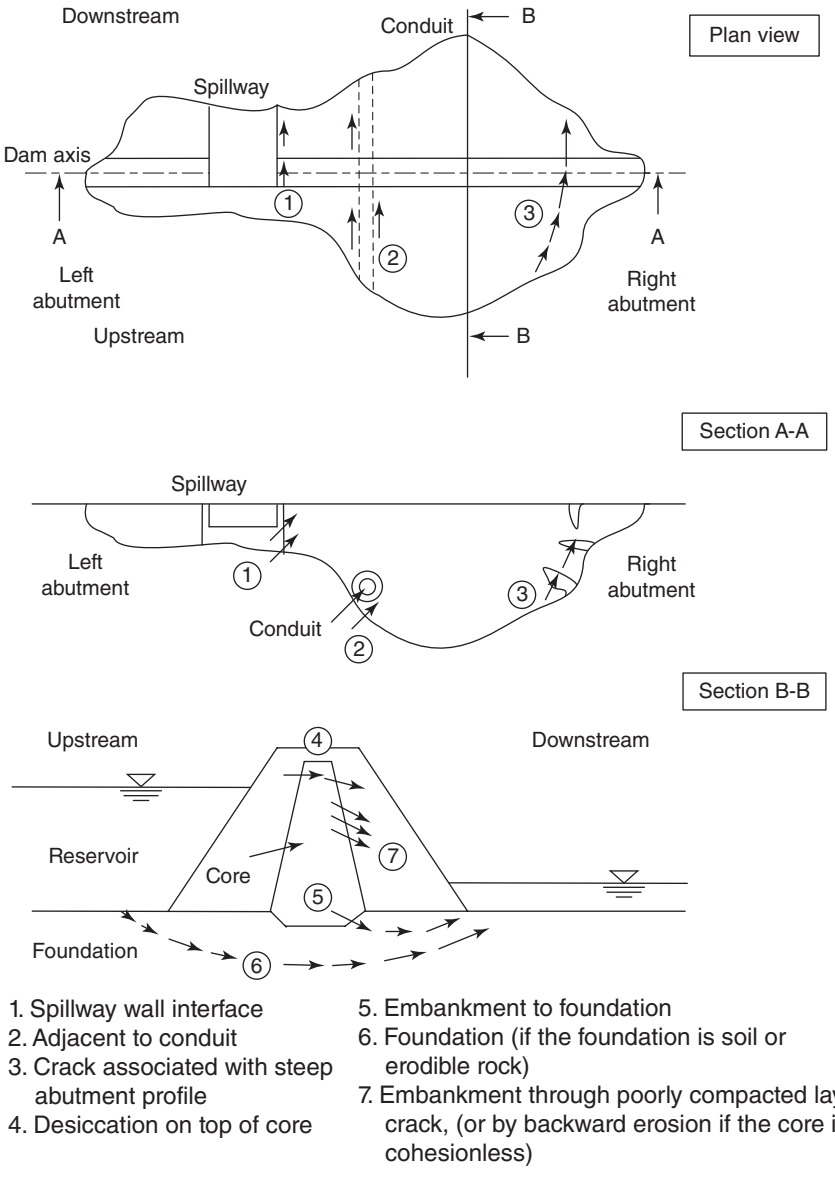

Figure 23.50 Possible locations of initiation of internal erosion. (After Fell and Fry 2005)

Values of i_{cr} typically vary in the range of 0.85 to 1.2. The hydraulic gradient in dams depends on many factors, including the difference in water level between the upstream and the downstream, the length of the drainage path, and the relative hydraulic conductivity of the various zones. The target maximum gradient in the flow must be kept much lower than the critical value, especially in areas where internal erosion is possible. Figure 23.53 shows ranges of hydraulic gradient values that are associated with initiation of internal erosion on the one hand and full development of piping on the other for unfiltered exit faces. Generally speaking, there is a trend toward higher-porosity soils beginning to erode at lower hydraulic gradients, even lower than 0.3. Yet, soils with plastic fines erode at higher gradients, and gap-graded soils begin to erode at lower gradients than nongap-graded soils with the same fine content. The U.S. Army Corps of Engineers uses a lower-bound value of the critical hydraulic gradient equal to 0.8 and allows a hydraulic gradient of up to 0.5 at the toe of levees, provided a number of conditions are met (USACE 2003). Another way to address the incipient motion of soil particles in internal erosion problems is to use the concept of critical velocity and charts such as Figure 23.8 and 23.9. However, these critical velocities were developed from sheet flow tests, and the critical velocity may be different from those initiating internal erosion.

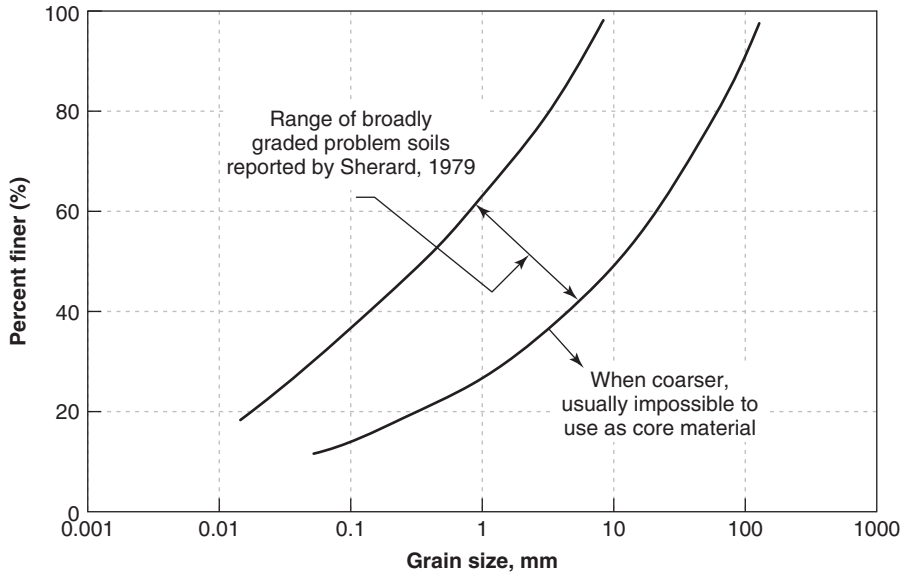

Figure 23.51 Range of problem soils for internal erosion. (After Sherard 1979)

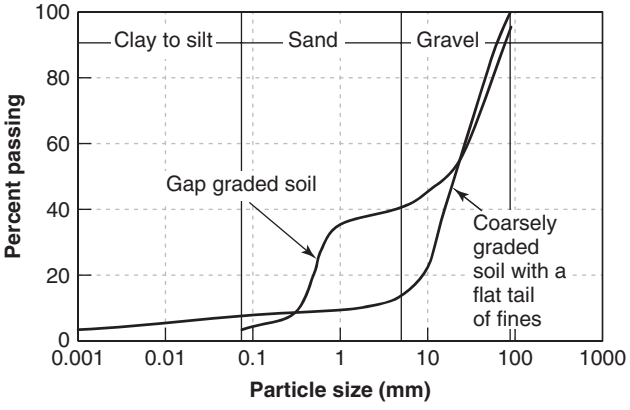

Figure 23.52 Range of problem soils for suffusion. (After Fell and Fry 2005)

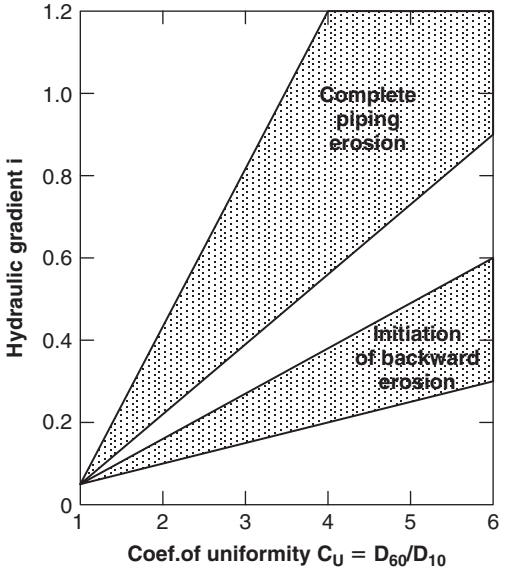

Figure 23.53 Range of hydraulic gradient values associated with internal erosion. (After Prezlmaier 2005)

Several methods, based in part on the analysis of the grain size curve, have been developed to evaluate the instability of soils in dams and their sensitivity to the suffusion phenomenon. They include Sherard (1979), Kenney and Lau (1986), Burenkova (1993), and Fell and Wan (2005).

23.12.4 Remedial Measures

Internal erosion of earth dams often occurs very quickly, leaving limited time for remedial action (Foster et al. 2000a, 2000b). Most of the time, complete breach occurs within 12 hours of first visual detection of internal erosion and sometimes in less than 6 hours. The majority of failures occur during the first filling or within 5 years after first filling. The process of suffusion tends to develop more slowly than the back erosion and piping processes.

One solution to many internal erosion problems is the use of quality filters. A *filter* is a layer of soil placed between a fine-grained soil and a coarse-grained soil to transition the flow without having the fines of the fine-grained soil erode through the voids of the coarse-grained soil. The grain size distribution curve of the soil filter layer is designed to provide this transition in a gradual fine-to-coarse fashion.

PROBLEMS

23.1 If a faucet drips on a pebble for 20 million years, will there be a hole in the pebble?

23.2 Water flows in a river at a mean depth shear velocity of 2 m/s. The gradient of the shear velocity at the bottom of the river is 7000 m/s per m of depth. Calculate the shear stress applied by the water to the bottom of the river. The soil particles at the bottom of the river are cubes 1 mm in size. They have a unit weight of 26.5 kN/m^3 and a friction angle equal to 35°. Calculate the shear stress necessary to move the soil grains. Compare this shear stress to the shear stress applied by the water; will there be erosion?

23.3 The particle of problem 2 is now a 1 mm diameter sphere that rests between two other spherical particles (Figure 23.1s). The particle is subjected to the same shear stress as in problem 2. Will the particle be able to roll over its neighbors and erode away?

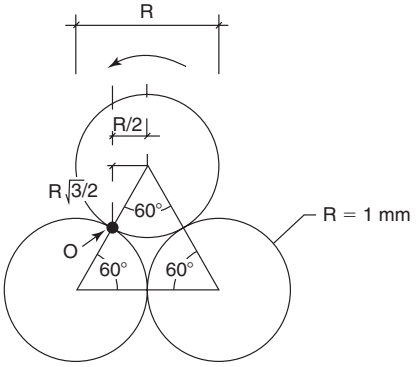

Figure 23.1s Soil particle.

23.4 The straight part of a river is at flood stage and experiences a 160-year flood. During the flood, the water depth is 6 m and the mean depth water velocity is 3 m/s. The bottom of the river is made of sand and the banks have a bank angle of 30°. Would you expect the sand to erode? If yes, what size rip rap would you recommend to place on top of the sand to prevent erosion? Would you place a geosynthetic filter between the sand and the rip rap? Explain.

23.5 A bridge is designed for a life of 50 years and you wish to design the bridge for a flood that has a probability of occurring or being exceeded of 0.001. What should the recurrence interval of the design flood be?

23.6 A round-nose pier is 3 m wide and 6 m long. The center-to-center spacing of the piers is 50 m. The water depth at the site is 10 m and the approach flow velocity of 3 m/s has an attack angle equal to 10° (Figure 23.2s). EFA tests were conducted; the average erosion function representing the soil is given in Figure 23.3s. The critical velocity of the soil is 1.6 m/s. The duration of the flood is 48 hours. Find the pier scour depth after 48 hours.

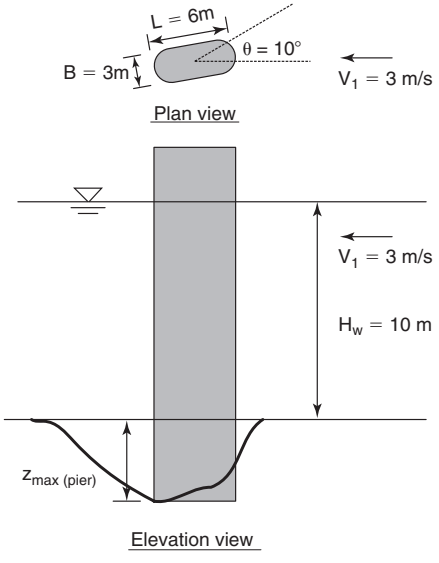

Figure 23.2s Pier scour problem.

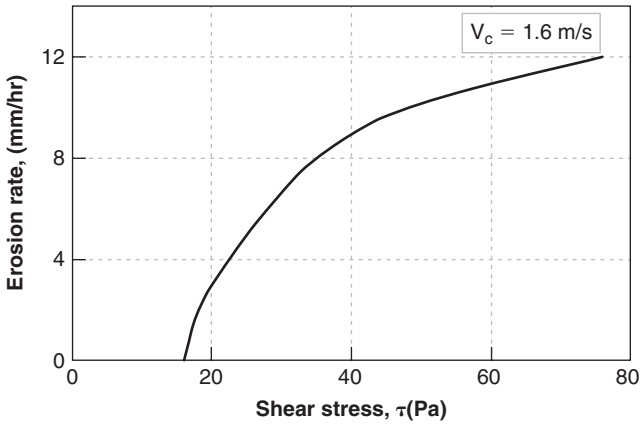

Figure 23.3s Erosion function.

23.7 Calculate the abutment and contraction scour depth after 48 hours of flood for the following case. The geometry of the channel and the bridge are given in Figure 23.4s. The compound channel is symmetrical, and the discharge during the flood is Q = 2000 m^3/s. The critical velocity of the soil in the main channel and flood plain is 1.2 m/s. The erosion function of the soil from an EFA test is given in Figure 23.5s. The duration of flood is 48 hours, and the hydraulic data are as follows:

Mean velocity in the general approach cross section: $V_1 = 1.13$ m/s
Mean velocity in the approach floodplain: $V_{f1} = 0.78$ m/s
Mean velocity in the approach main channel: $V_{m1} = 1.4$ m/s
Water depth in the approach flood plain: $H_{wf1} = 2.55$ m
Water depth in the approach main channel: $H_{wm1} = 7.9$ m
Mean velocity in the general contracted cross section: $V_2 = 1.75$ m/s
Mean velocity in the contracted main channel: $V_{m2} = 1.83$ m/s
Hydraulic radius in the approach main channel: $R_{h1} = 3.65$ m
Find the abutment scour depth and the contraction scour depth after 48 hours of flood.

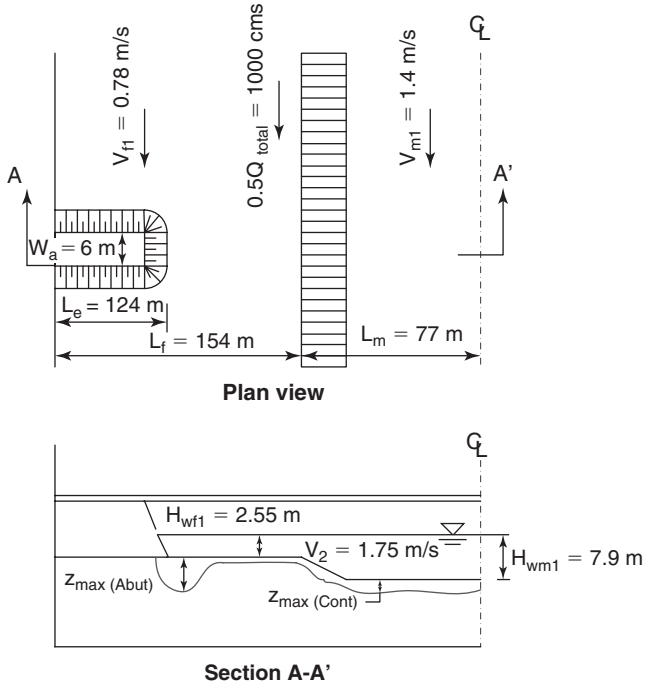

Figure 23.4s Channel geometry.

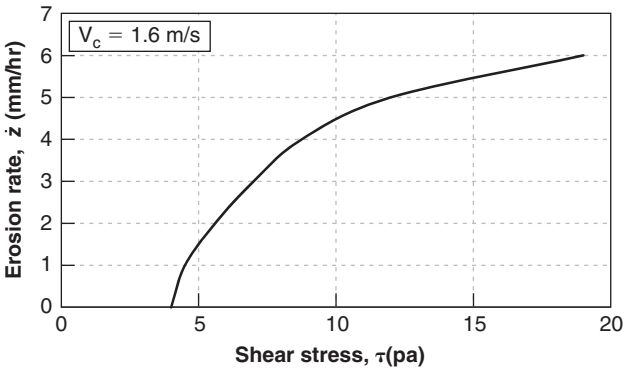

Figure 23.5s Erosion function.

23.8 Download the SRICOS-EFA program from the web site http://ceprofs.tamu.edu/briaud/ and run Example 1 from the list of examples.

23.9 Download the MEANDER program from the web site http://ceprofs.tamu.edu/briaud/ and run Example 1 from the list of examples.

23.10 A 5 m high levee is overtopped for 2 hours during a hurricane. The levee material and the soil below the levee are borderline between a high-plasticity clay CH and a low-plasticity clay CL. Draw a contour of the levee after 2 hours of overtopping.

23.11 Repeat problem 23.10 for a flood that lasts 72 hours.

Problems and Solutions

Problem 23.1

If a faucet drips on a pebble for 20 million years, will there be a hole in the pebble?

Solution 23.1

Common sense might lead you to say yes. Then the question might become: How is it possible for a stress level as small as the one created by a drop of water to destroy the bonds of the rock? The answer may be that any stress, no matter how small, can defeat any strength, no matter how large, provided the number of cycles is high enough. Experiments to check such a statement would be very valuable.

Problem 23.2

Water flows in a river at a mean depth shear velocity of 2 m/s. The gradient of the shear velocity at the bottom of the river is 7000 m/s per m of depth. Calculate the shear stress applied by the water to the bottom of the river. The soil particles at the bottom of the river are cubes 1 mm in size. They have a unit weight of 26.5 kN/m^3 and a friction angle equal to 35°. Calculate the shear stress necessary to move the soil grains. Compare this shear stress to the shear stress applied by the water; will there be erosion?

Solution 23.2

From the problem statement:

$$v = 2 \text{ m/s}$$

$$\frac{dv}{dz} = \frac{7000 \text{ m/s}}{\text{m}}$$

Particle size: 1 mm cube

$$\gamma_s = 26.5 \text{ kN/m}^3$$

$$\mu = 1 \times 10^{-3} \text{ Pa} \cdot \text{s}$$

a. Shear stress applied by the water at the bottom of the river:

$$\tau_w = \mu\left(\frac{dv}{dz}\right) = (1 \times 10^{-3}\ \text{Pa}\cdot\text{s}) \times \left(7000\ \frac{\text{m/s}}{\text{m}}\right) = 7\ \text{Pa}$$

b. Shear stress necessary to move the grains:

$$\tau_s = \sigma_N \times \tan\varphi' = \left(\frac{\gamma_s \times V}{\text{A}}\right) \times \tan\varphi' = \left(\frac{26500 \times 10^{-9}}{10^{-6}}\right) \times \tan 35 = 18.56\ \text{Pa}$$

c. Comparison:

Stress necessary to move the grains ($\tau_s = 18.56$ Pa) is larger than the shear stress generated by the water ($\tau_w = 7$ Pa); therefore, there will be no erosion.

Problem 23.3

The particle of problem 2 is now a 1 mm diameter sphere that rests between two other spherical particles (Figure 23.1s). The particle is subjected to the same shear stress as in problem 2. Will the particle be able to roll over its neighbors and erode away?

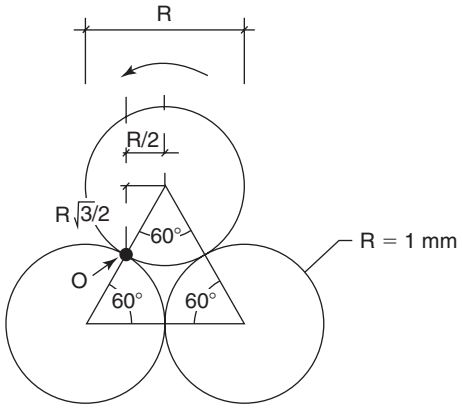

Figure 23.1s Soil particle.

Solution 23.3

The driving moment M_D and resisting moment M_R around point O in Figure 23.1s are calculated. For the driving moment, it is assumed that the drag force exerted by the shear stress acts on the projected surface of the spherical particle and that the normal stress applied by the water due to the flow is negligible:

$$M_D = \tau_w \frac{\pi D^2}{4}\left(R + \frac{\sqrt{3}R}{2}\right) = 7 * 10^{-6} * \frac{\pi}{4} * 1^2(1 + 0.87) = 10.25 * 10^{-6}\ \text{N.mm}$$

$$M_R = W\frac{R}{2} = \gamma_s V\frac{R}{2} = \frac{26500}{10^9} * \frac{4}{3}\pi D^3 * \frac{0.5}{2} = 27.74 * 10^{-6}\ \text{N.mm}$$

$M_R > M_D \rightarrow$ The particle won't be able to roll over its neighbors and erode away

Problem 23.4

The straight part of a river is at flood stage and experiences a 160-year flood. During the flood, the water depth is 6 m and the mean depth water velocity is 3 m/s. The bottom of the river is made of sand and the banks have a bank angle of 30°. Would you expect the sand to erode? If yes, what size rip rap would you recommend to place on top of the sand to prevent erosion? Would you place a geosynthetic filter between the sand and the rip rap? Explain.

Solution 23.4

Yes, one would expect the sand to erode. Indeed, the water velocity is 3 m/s and the critical velocity of the sand will be at most 1 m/s (Figure 23.8).

Rip rap can be sized as follows:

$$d_{30} = H_w F\, C_{st} C_v C_t \left(\frac{V_{des}}{\sqrt{C_{sl}\left(G_s - 1\right) g H_w}} \right)^{2.5}$$

The height of water is 6 m and we choose a factor of safety equal to 2. Also, we assume that the rip rap blocks are angular, so C_{st} is equal to 0.3.

The magnitude of C_{sl} is calculated with $\theta = 30^\circ$:

$$C_{sl} = \sqrt{1 - \left(\frac{\sin\left(\theta - 14^\circ\right)}{\sin 32^\circ} \right)^{1.6}} = \sqrt{1 - \left(\frac{\sin 16^\circ}{\sin 32^\circ} \right)^{1.6}} = 0.8$$

$$d_{30} = 6 \times 2 \times 0.3 \times 1.23 \times 1 \left(\frac{3}{\sqrt{0.8\,(2.65 - 1)\,9.81 \times 6}} \right)^{2.5} = 0.3 \text{ m}$$

It is very important to place a filter between the soil to be protected and the rip-rap layer. Without a filter, the soil under the rip rap may continue to erode through the large voids in the rip rap; in the end, the rip rap may not move away, but may simply go down significantly as the underlying soil erodes away.

Problem 23.5

A bridge is designed for a life of 50 years and you wish to design the bridge for a flood that has a probability of occurring or being exceeded of 0.001. What should the recurrence interval of the design flood be?

Solution 23.5

$$R = 1 - \left(1 - \frac{1}{T_R}\right)^{L_t}$$

where T_R is the return period and R is the probability of exceedance of the flood.

$$0.001 = 1 - \left(1 - \frac{1}{T_R}\right)^{50} \rightarrow \left(1 - \frac{1}{T_R}\right)^{50} = 0.999$$

$$50 \times \log\left(1 - \frac{1}{T_R}\right) = \log 0.999$$

$$\log\left(1 - \frac{1}{T_R}\right) = \frac{-4.34512 \times 10^{-4}}{50} = -8.690 \times 10^{-6}$$

$$1 - \frac{1}{T_R} = 0.99997999 \rightarrow T_R = 50000 \text{ yrs.}$$

The 50,000-year flood is the one to be considered.

Problem 23.6

A round-nose pier is 3 m wide and 6 m long. The center-to-center spacing of the piers is 50 m. The water depth at the site is 10 m and the approach flow velocity of 3 m/s has an attack angle equal to 10° (Figure 23.2s). EFA tests were conducted; the average erosion function representing the soil is given in Figure 23.3s. The critical velocity of the soil is 1.6 m/s. The duration of the flood is 48 hours. Find the pier scour depth after 48 hours.

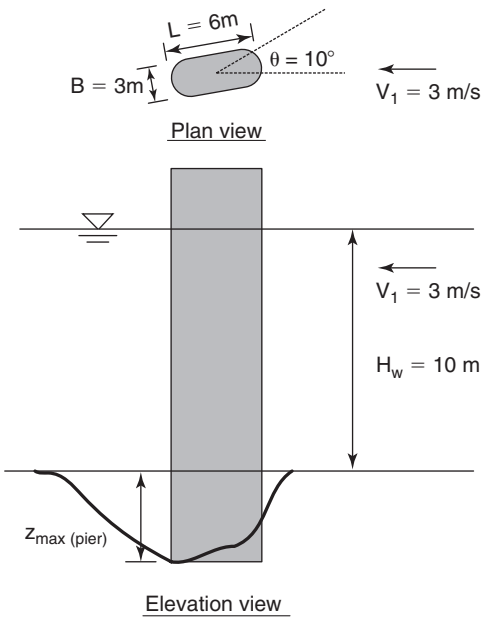

Figure 23.2s Pier scour problem.

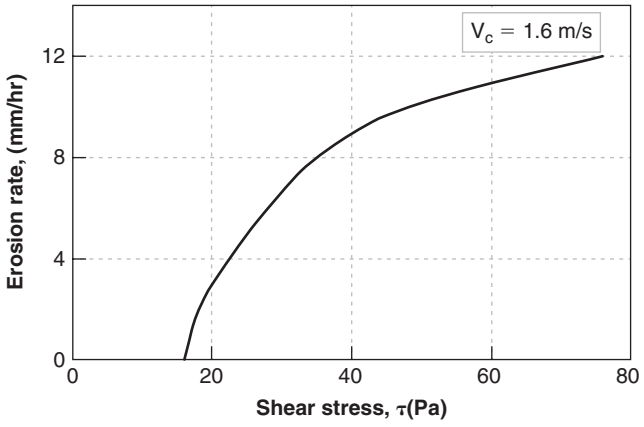

Figure 23.3s Erosion function.

Solution 23.6

The maximum scour depth and the maximum shear stress around the pier can be calculated as follows.

Maximum Scour Depth

The correction factors for water depth (K_{pw}), pier shape (K_{psh}), pier aspect ratio (K_{pa}), and pier spacing (K_{psp}) must be calculated first:

$$K_{pw} = \begin{cases} 0.89\left(\dfrac{h_w}{B'}\right)^{0.33}, & \text{for } \dfrac{h_w}{B'} < 1.43 \\ 1.0 \quad\quad\quad\quad\quad , & \text{else} \end{cases}$$

$$B' = B\left(\cos\theta + \frac{L}{B}\cdot\sin\theta\right) = 3\left(\cos 10 + \frac{6}{3}\sin 10\right) = 4 \text{ m}$$

$$\frac{h_w}{B'} = \frac{10}{4} = 2.5 > 1.43 \quad so \quad K_{pw} = 1$$

$\mathrm{K_{psh}} = 1$ because the pier has a round nose

$\mathrm{K_{l/B}} = 1$ because the projected width has been used.

$$K_{psp} = \begin{cases} 2.9\left(\dfrac{S}{B'}\right)^{-0.91} & , \text{ for } \dfrac{S}{B'} < 3.42 \\ 1.0 & , \text{ else} \end{cases}$$

$$\frac{S}{B'} = \frac{50}{4} = 12.5 > 3.42 \quad so \quad K_{psp} = 1$$

All correction factors are equal to 1.0. The Froude Number is calculated with the approach velocity and pier width:

$$Fr_{(\text{pier})} = \frac{V_1}{\sqrt{g \cdot B'}} = \frac{3}{\sqrt{9.81 \times 4}} = 0.48$$

The critical pier Froude Number is calculated:

$$Fr_{c(\text{pier})} = \frac{V_c}{\sqrt{g \cdot B'}} = \frac{1.6}{\sqrt{9.81 \times 4}} = 0.255$$

Therefore, the maximum pier scour depth in given condition is:

$$\begin{aligned} z_{\max(\text{Pier})} &= 2.2 \cdot K_{pw} \cdot K_{psh} \cdot K_{pa} \cdot K_{psp} \cdot a' \cdot (2.6 Fr_{(\text{pier})} - Fr_{c(\text{pier})})^{0.7} \\ &= 2.2 \times 1 \times 1 \times 1 \times 1 \times 4 \times (2.6 \times 0.480 - 0.255)^{0.7} = 8.757 \text{ m} \\ &= 8757 \text{ mm} \end{aligned}$$

Maximum Shear Stress around Pier

The correction factors for water depth (k_{pw}) and for pier spacing (k_{psp}) are calculated and found equal to 1. For pier shape,

$$k_{psh} = 1.15 + 7e^{(-4L/a)} = 1.15 + 7e^{(-4\times 6/2)} = 1.15$$

The angle of attack factor is:

$$k_{psk} = 1 + 1.5\left(\frac{\theta}{90}\right)^{0.57} = 1 + 1.5\left(\frac{10}{90}\right)^{0.57} = 1.429$$

The Reynolds Number based on pier width is:

$$R_e = \frac{VD}{\nu} = \frac{3 \times 4}{10^{-6}} = 12000000$$

Therefore, the maximum shear stress around the pier in the given condition is:

$$\begin{aligned} \tau_{\max(\text{Pier})} &= k_{pw} \times k_{psh} \times k_{psp} \times k_{psk} \times 0.094 \rho {V_1}^2 \left(\frac{1}{\log R_e} - \frac{1}{10}\right) \\ &= 1 \times 1.15 \times 1 \times 1.429 \times 0.094 \times 1000 \times 3^2 \left(\frac{1}{\log 12000000} - \frac{1}{10}\right) \\ &= 57.36 \text{ Pa} \end{aligned}$$

Initial Rate of Scour

$\dot{z}_{i(\text{pier})}$ is read on the EFA curve at $\tau = \tau_{\max}$, and is 10.25 mm/hr (Figure 23.6s).

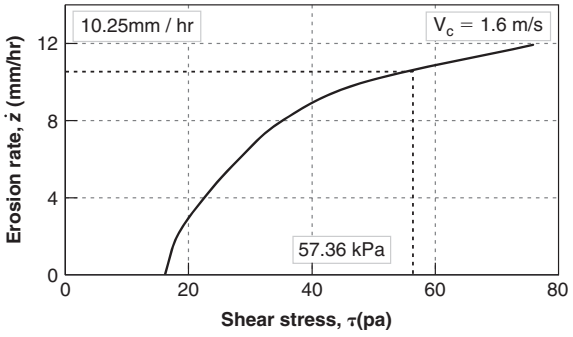

Figure 23.6s Erosion function and initial erosion rate for pier scour.

The depth of pier scour after the 48-hour duration of the 160-year flood can be calculated as:

$$z_{final}(t) = \frac{t\,(hrs)}{\dfrac{1}{\dot{z}_i} + \dfrac{t\,(hrs)}{y_{s\,(\max)}}} = \frac{48}{\dfrac{1}{10.2} + \dfrac{48}{8757}} = 463.7 \text{ mm}$$

Problem 23.7

Calculate the abutment and contraction scour depth after 48 hours of flood for the following case. The geometry of the channel and the bridge are given in Figure 23.4s. The compound channel is symmetrical, and the discharge during the flood is $Q = 2000\,m^3/s$. The critical velocity of the soil in the main channel and flood plain is 1.2 m/s. The erosion function of the soil from an EFA test is given in Figure 23.5s. The duration of flood is 48 hours, and the hydraulic data are as follows:

Mean velocity in the general approach cross section: $V_1 = 1.13$ m/s
Mean velocity in the approach floodplain: $V_{f1} = 0.78$ m/s
Mean velocity in the approach main channel: $V_{m1} = 1.4$ m/s
Water depth in the approach flood plain: $H_{wf1} = 2.55$ m
Water depth in the approach main channel: $H_{wm1} = 7.9$ m
Mean velocity in the general contracted cross section: $V_2 = 1.75$ m/s
Mean velocity in the contracted main channel: $V_{m2} = 1.83$ m/s
Hydraulic radius in the approach main channel: $R_{h1} = 3.65$ m

Find the abutment scour depth and the contraction scour depth after 48 hours of flood.

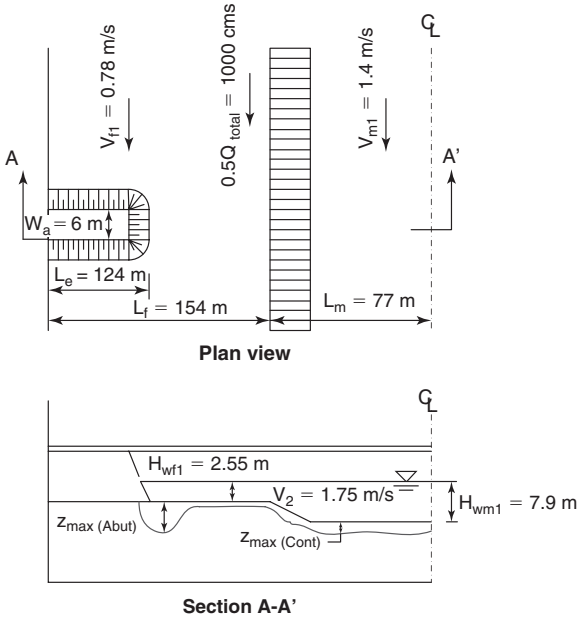

Figure 23.4s Channel geometry.

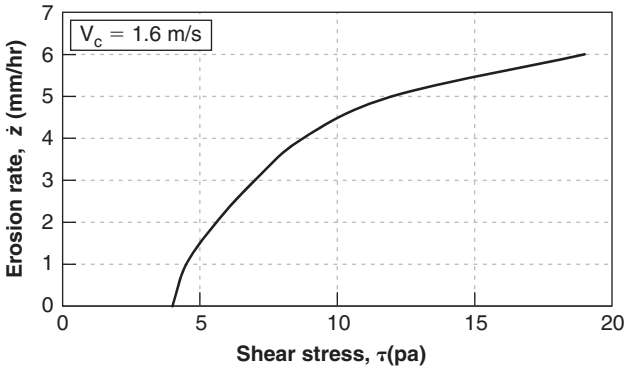

Figure 23.5s Erosion function.

Solution 23.7

Step 1. Calculate the maximum shear stress in the middle of the channel and around the abutment

Contraction scour

The maximum shear stress in the middle of the channel can be calculated as:

$$\tau_{\max(\text{Cont})} = k_{cr}k_{cl}k_{c\theta}k_{cw}\gamma n^2 {V_1}^2 {R_h}^{-1/3}$$

where k_{cr} is the correction factor for the contraction ratio, k_{cl} is the correction factor for the contraction length, $k_{c\theta}$ is the correction factor for the transition angle, and k_{cw} is the correction factor for the water depth.

For this case,

$$k_{cr} = 0.62 + 0.38\left(\frac{A_1}{A_2}\right)^{1.75} = 0.62 + 0.38 \times \left(\frac{V_2}{V_1}\right)^{1.75} = 0.62 + 0.38 \times \left(\frac{1.75}{1.13}\right)^{1.75} = 1.44$$

Width of the channel at approach section:

$$L_1 = (154 + 77) \times 2 = 462 \text{ m}$$

Width of the channel at contraction section:

$$L_2 = (30 + 77) \times 2 = 214 \text{ m}$$

$$k_{cl} = 0.77 + 1.36\left(\frac{6}{462 - 214}\right) - 1.98\left(\frac{6}{462 - 214}\right)^2 = 0.80$$

$$k_{c\theta} = 1 + 0.9\left(\frac{90}{90}\right)^{1.5} = 1.9$$

$$k_{cw} = 1$$

Therefore,

$$\tau_{\max(\text{Cont})} = k_{cr}k_{cl}k_{c\theta}k_{cw}\gamma n^2 {V_1}^2 {R_h}^{-1/3} = 1.44 \times 0.80 \times 1.9 \times 1 \times 9810 \times 0.018^2 \times 1.13^2 \times 3.65^{-1/3}$$
$$= 5.77 \text{ Pa}$$

Abutment scour

The maximum shear stress around the abutment can be calculated as:

$$\tau_{\max(\text{Abut})} = 12.45 \times k_{acr} \times k_{ash} \times k_{aw} \times k_{as} \times k_{ask} \times k_{al} \times \rho \times {V_1}^2 \times \text{Re}^{-0.45}$$

where k_{acr} is the contraction ratio influence factor for abutment scour shear stress, k_{ash} is the correction factor for aspect ratio of the approach embankment, k_{aw} is the correction factor for Froude Number, k_{as} is the correction factor for abutment shape, k_{ask} is the correction factor for the skew angle of the abutment, and k_{al} is the correction factor for abutment location in the flood plain.

For this case:

$$k_{acr} = 3.65\frac{q_2}{q_1} - 2.91 = 3.65 \times \frac{1.75}{1.13} - 2.91 = 2.74$$

$$k_{ash} = 0.85\left(\frac{L_e}{W_a}\right)^{-0.24} = 0.85 \times \left(\frac{124}{6}\right)^{-0.24} = 0.41$$

$$Fr = \frac{V_1}{\sqrt{gH_{wf1}}} = \frac{1.13}{\sqrt{9.81 \times 2.55}} = 0.23 > 0.1$$

Therefore,

$$k_{aw} = 2.07Fr + 0.8 = 2.07 \times 0.23 + 0.8 = 1.27$$

Because this is a spill-through abutment,

$$k_{as} = 0.58$$

$$k_{ask} = 1$$

Because

$$\frac{L_f - L_e}{H_{wf1}} = \frac{154 - 124}{2.55} = 11.76 > 1, k_{al} = 1$$

Therefore,

$$\begin{aligned}\tau_{\max(\text{Abut})} &= 12.45 \times k_{acr} \times k_{ash} \times k_{aw} \times k_{as} \times k_{ask} \times k_{al} \times \rho \times {V_1}^2 \times \text{Re}^{-0.45} \\ &= 12.45 \times 2.74 \times 0.41 \times 1.27 \times 0.58 \times 1 \times 1 \times 1000 \times 1.13^2 \times \left(\frac{1.13 \times 6}{10^{-6}}\right)^{-0.45} \\ &= 11.09 \text{ Pa}\end{aligned}$$

The initial rate of scour z_i for contraction scour and abutment scour are read on the EFA curve at $\tau = \tau_{\max}$: it is 2.01 mm/hr and 4.7 mm/hr respectively as shown in Figure 23.7s.

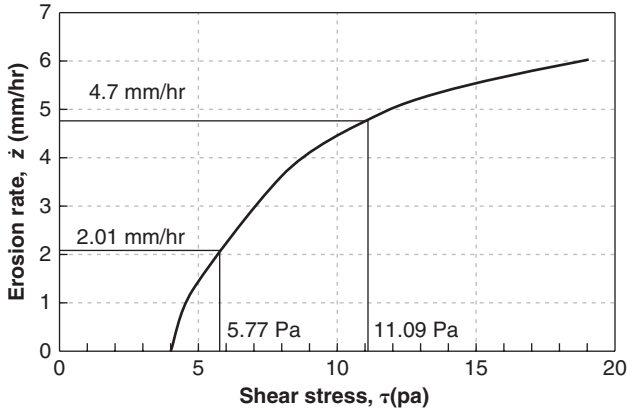

Figure 23.7s Erosion function and initial erosion rate for abutment scour and contraction scour.

Step 2. Calculate the maximum contraction scour depth and the maximum abutment scour depth

Contraction scour

The maximum contraction scour depth can be calculated as:

$$z_{\max(\text{Cont})} = 1.27(1.83Fr_{m2} - Fr_{mc}) \cdot H_{wm1}$$

where Fr_{m2} is the Froude Number for the main channel at the bridge in the contracted zone, Fr_{mc} is the critical Froude Number for the main channel at the bridge, and H_{wm1} is the water depth in the main channel at the approach section.

For this case,

$$Fr_{m2} = \frac{V_1/CR}{\sqrt{gH_{wm1}}} = \frac{V_2}{\sqrt{gH_{wm1}}} = \frac{1.75}{\sqrt{9.81 \times 7.9}} = 0.199$$

$$Fr_{mc} = \frac{V_{mc}}{\sqrt{gH_{wm1}}} = \frac{1.2}{\sqrt{9.81 \times 7.9}} = 0.136$$

Therefore,

$$y_{\text{s(Cont)}} = 1.27(1.83Fr_{m2} - Fr_{mc}) \cdot H_{wm1} = 1.27 \times (1.83 \times 0.199 - 0.136) \times 7.9 = 2.29 \text{ m}$$

Abutment scour

The maximum abutment scour depth can be calculated as:

$$y_{s(\text{Abut})} = H_{wf1} \cdot K_{ash} \cdot K_{ask} \cdot K_{al} \cdot K_{ag} \cdot 243 \cdot \text{Re}_{f2}{}^{-0.28}(1.65Fr_{f2} - Fr_{fc})$$

where K_{ash} is the correction factor for the abutment shape, K_{ask} is the correction factor for the abutment skew, K_{al} is the influence factor that takes into account the proximity of the abutment to the main channel, K_{ag} is the geometry of the channel influence factor for abutment scour, Re_{f2} is the Reynolds Number around the toe of the abutment, Fr_{f2} is the Froude Number around the toe of the abutment, and Fr_{fc} is the critical Froude Number for soil near the toe of the abutment.

For this case, assume that it is a spill-through abutment with 2:1 slope, $K_{ash} = 0.73$

$$K_{ask} = 1 - 0.005|\theta - 90| = 1$$

For this compound channel, $K_{ag} = 1$

Because

$$\frac{L_f - L_e}{H_{wf1}} = \frac{154 - 124}{2.55} = 11.8 > 1.5$$

therefore, $K_{al} = 1$

Because

$$\frac{L_f - L_e}{H_{wm1}} = \frac{154 - 124}{7.9} = 3.8 < 5$$

it is a short setback condition. Therefore,

$$V_{f2} = \frac{0.5Q}{A_2} = 0.5 \times V_2 = 0.5 \times 1.75 = 0.875 \text{ m/s}$$

$$\text{Re}_{f2} = \frac{V_{f2} \cdot H_{wf1}}{\nu} = \frac{0.875 \times 2.55}{10^{-6}} = 2.23 \times 10^6$$

$$Fr_{f2} = \frac{V_{f2}}{\sqrt{gH_{wf1}}} = \frac{0.875}{\sqrt{9.81 \times 2.55}} = 0.175$$

$$Fr_{fc} = \frac{V_{fc}}{\sqrt{gH_{wf1}}} = \frac{1.2}{\sqrt{9.81 \times 2.55}} = 0.24$$

and thus

$$z_{\max(\text{Abut})} = H_{wf1} \cdot K_{ash} \cdot K_{ask} \cdot K_{al} \cdot K_{ag} \cdot 243 \cdot \text{Re}_{f2}{}^{-0.28}(1.65Fr_{f2} - Fr_{fc})$$
$$= 2.55 \times 0.73 \times 1 \times 1 \times 1 \times 243 \times (2.23 \times 10^6)^{-0.28}(1.65 \times 0.175 - 0.24) = 0.368 \text{ m}$$

Step 3. Calculate the depth of contraction scour and abutment scour after 48 hours

$$z_{(\text{Cont})}(t) = \frac{t(hrs)}{\frac{1}{\dot{z}_i} + \frac{t(hrs)}{z_{\max(\text{Cont})}}} = \frac{48}{\frac{1}{2.01} + \frac{48}{2290}} = 93 \text{ mm}$$

$$z_{\max(\text{Abut})}(t) = \frac{t(hrs)}{\frac{1}{\dot{z}_i} + \frac{t(hrs)}{y_{s(\text{Abut})}}} = \frac{48}{\frac{1}{4.7} + \frac{48}{368}} = 140 \text{ mm}$$

Therefore, the contraction scour depth generated by the 48-hour flood is 4.1% of the maximum contraction scour depth, whereas the abutment scour depth generated by the same flood is 38% of the maximum abutment scour depth.

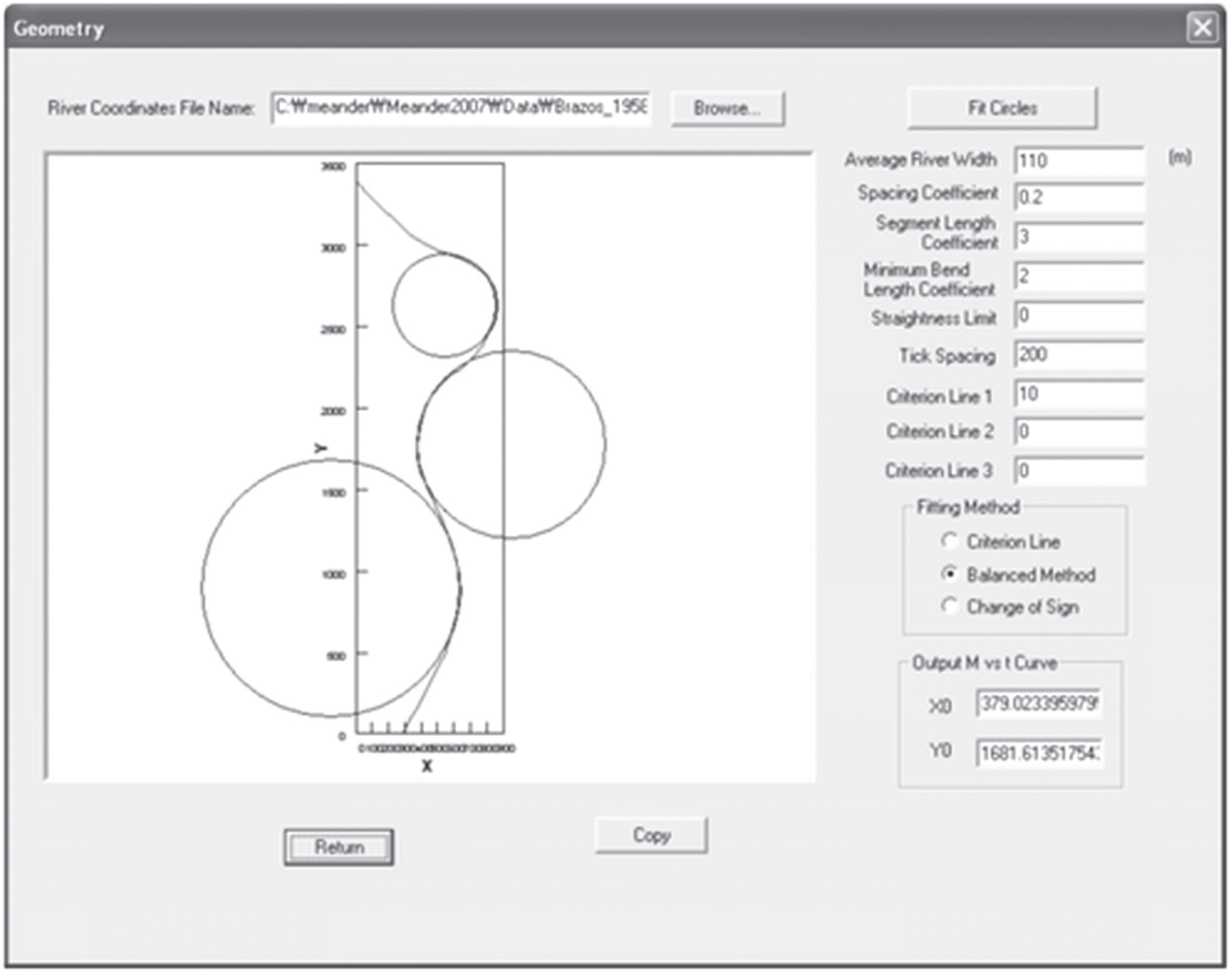

Figure 23.8s Input the geometry data.

Problem 23.8

Download the SRICOS-EFA program from the web site http://ceprofs.tamu.edu/briaud/ and run Example 1 from the list of examples.

Solution 23.8

See the web site.

Problem 23.9

Download the MEANDER program from the web site http://ceprofs.tamu.edu/briaud/ and run Example 1 from the list of examples.

Solution 23.9

1. Install MCRInstaller and run MEANDER.
2. Open the first example, Brazos1958C_const_NGP.meander, in the Data folder included with the program. This example is for migration with a constant discharge.
3. Choose between SI units or English units in Input > Units . . . . Choose the SI Units.
4. Open the *Geometry* window. This window lets you open the file with the initial coordinates of the river and fit circles that represent the meanders. Browse the geometry file Brazos_1958C_2006.dat included in the Data folder, which has the initial coordinates of the river.
5. The numbers in the *Geometry* window (Figure 23.8s) must be: Average River Width is 110 m, the Tick Spacing is 200, and the Criterion Lines 1, 2, and 3 are 10, 0, and 0 respectively. Click Fit Circles. Click Return after the circles are fitted.
6. The next window (Figure 23.9s) lets you input the data soil. Input the EFA curve on the *Soil Data* window and choose the sand option for the type of the soil.

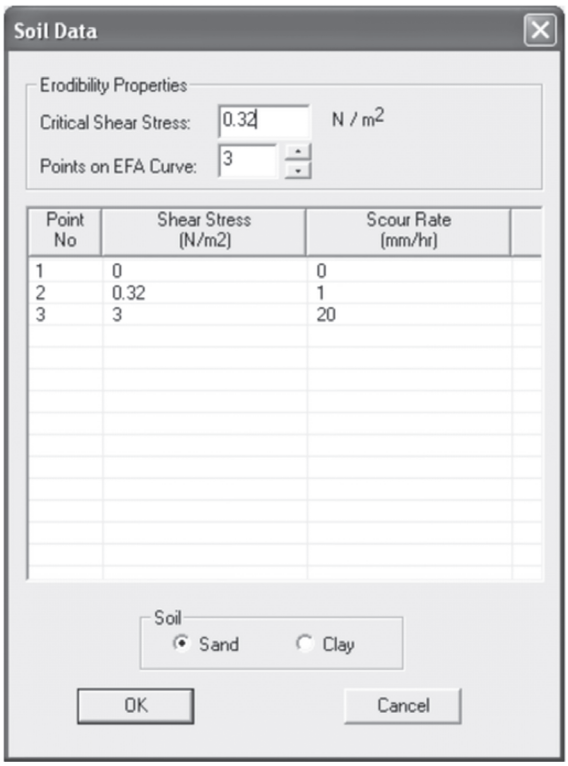

Figure 23.9s Soil data window.

7. Open the *Water Data* window (Figure 23.10s). The Critical Froude Number is 0.17 and the Time Step is 240. The speed of the program depends on this increment. The discharge, in the case of this example, is constant. The discharge units are in cubic meters per second. The time period is one year or 365 days. The discharge versus velocity and the discharge versus water depth have to be obtained from software such as HEC-RAS or TAMU-FLOW. These programs perform their analyses based on the cross section of the river. Click OK after you are done.
8. Before running the program, you may want to check the data again by clicking *Input Tables* and *Input Plots*. These two options let you review your data.
9. Once all the data are in, you can click the Run button. After the program finishes the calculations, click the *Output Plots* icon (Figure 23.11s). Click Center Line or One Bank to see the results of the meander migration (Figure 23.12s).

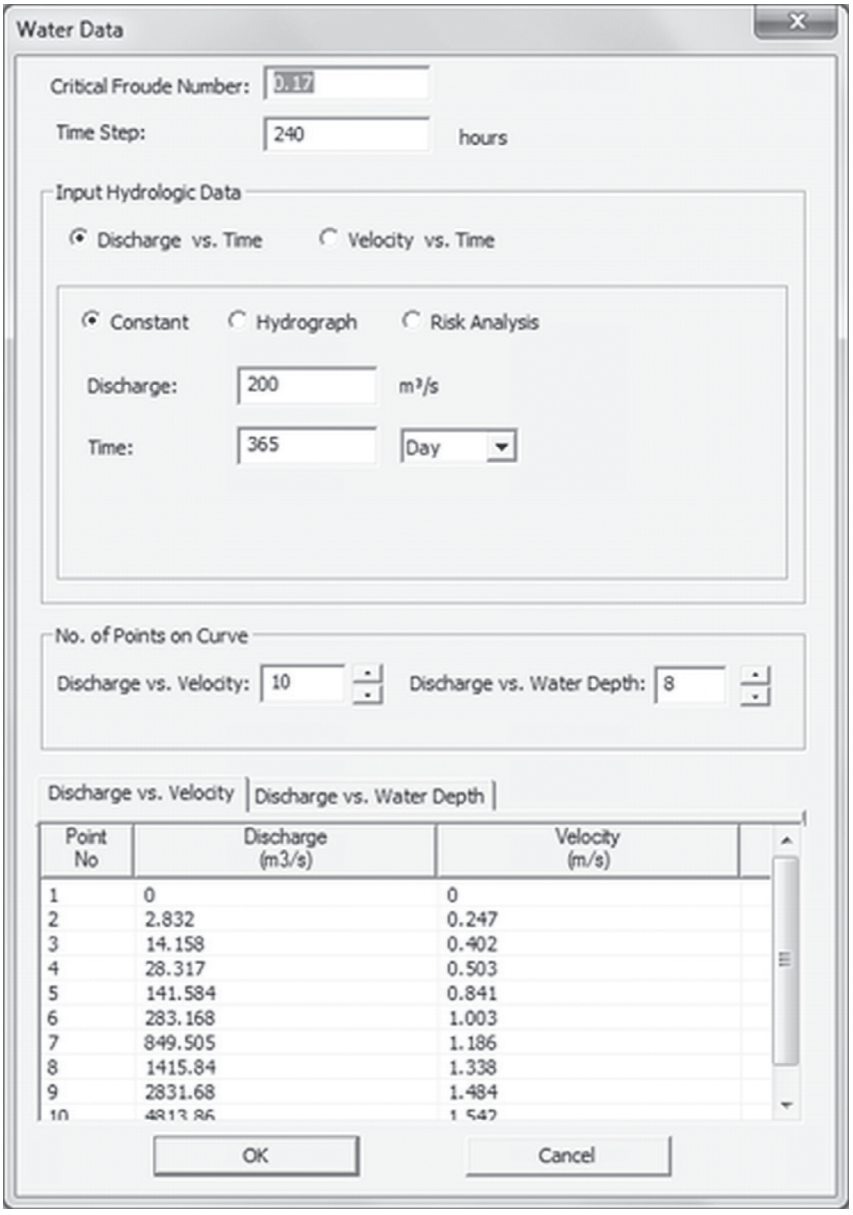

Figure 23.10s Water data input.

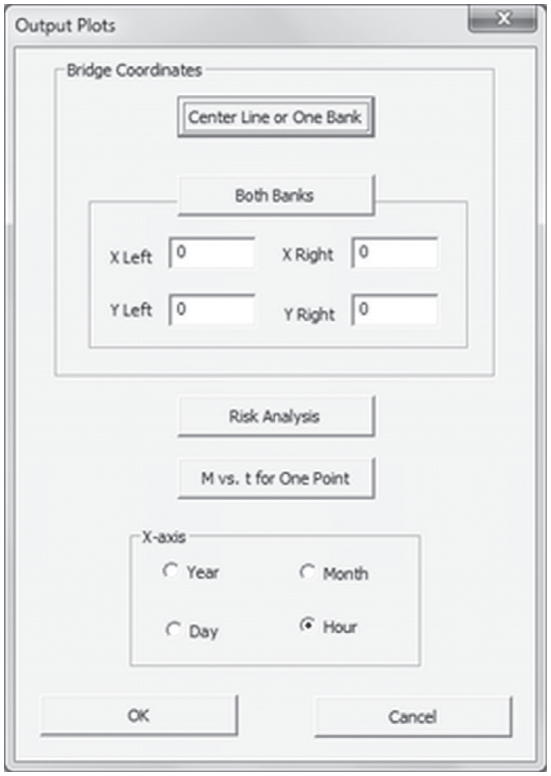

Figure 23.11s Output plots windows.

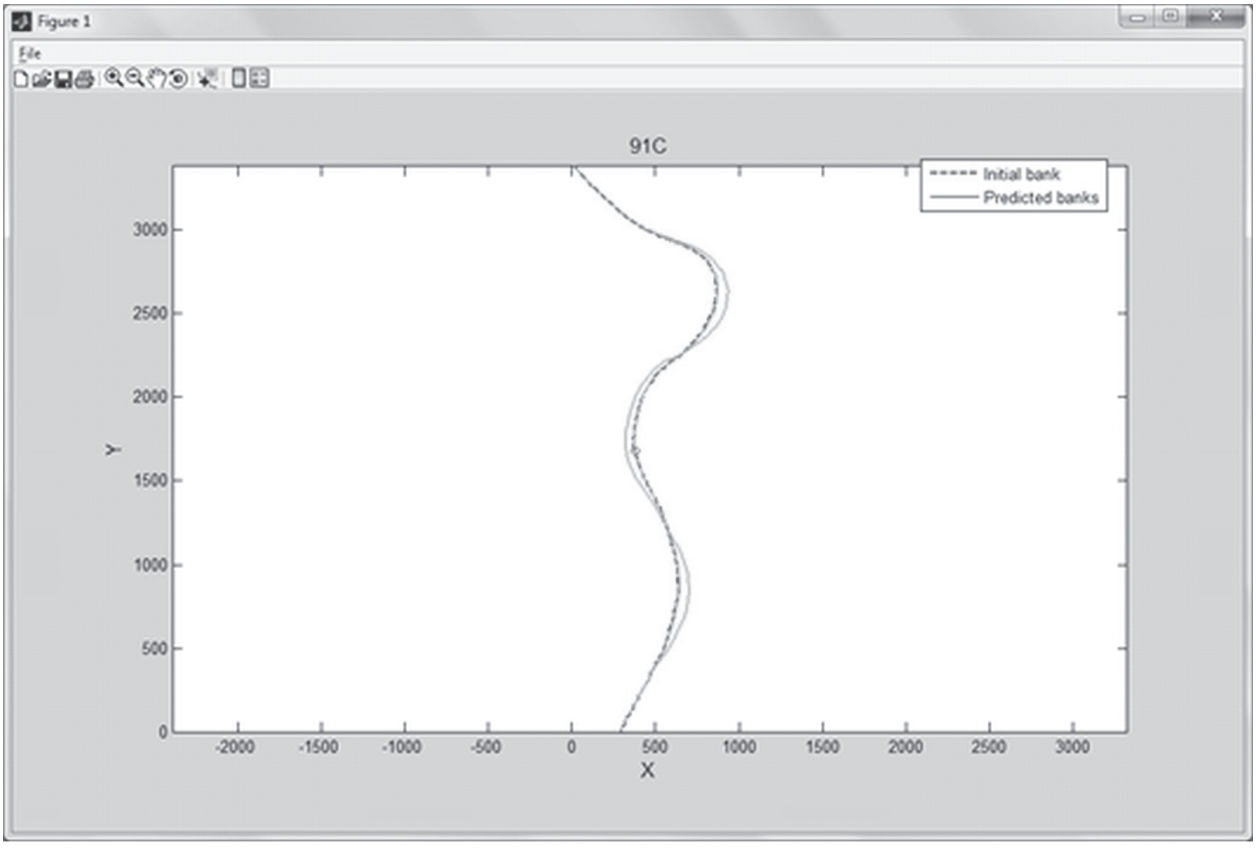

Figure 23.12s Results of the meander migration.

Problem 23.10

A 5 m high levee is overtopped for 2 hours during a hurricane. The levee material and the soil below the levee are borderline between a high-plasticity clay CH and a low-plasticity clay CL. Draw a contour of the levee after 2 hours of overtopping.

Solution 23.10

To draw the contour of the levee after 2 hours of overtopping erosion, we must first find where the erosion will start. When the water overtops the levee, it accelerates and reaches the critical velocity of the soil $Vc = 1.1$ m/s after some distance from the levee crest. This distance is such that:

$$V = \sqrt{2gH}$$

$$1.1 = \sqrt{2 \times 9.81 \times H} \rightarrow H = 0.06 \text{ m}$$

So, erosion will start once the water has reached a levee height equal to $5 - 0.06 \text{ m} = 4.94 \text{ m}$.

Then we select five points along the levee and compute the erosion after 2 hours (problem 23.10) and after 72 hours (problem 23.11). To calculate the erosion depth, we first calculate the water velocity, then find the corresponding erosion rate from the erosion function, and then multiply the erosion rate by the overtopping duration (2 or 72 hours). The levee soil is borderline between a high-plasticity clay CH and a low-plasticity clay CL, so the erosion function is selected as the boundary line on the erosion chart of Figure 23.13s. Example calculations are shown for a depth of 4 m below the crest of the levee.

$H = 4$ m

$V = \sqrt{2gH} = \sqrt{2 \times 9.81 \times 4} = 8.86$ m/s $\rightarrow$ erosion rate = 58 mm/hr

Erosion depth $z = 58 \times 2 = 116$ mm

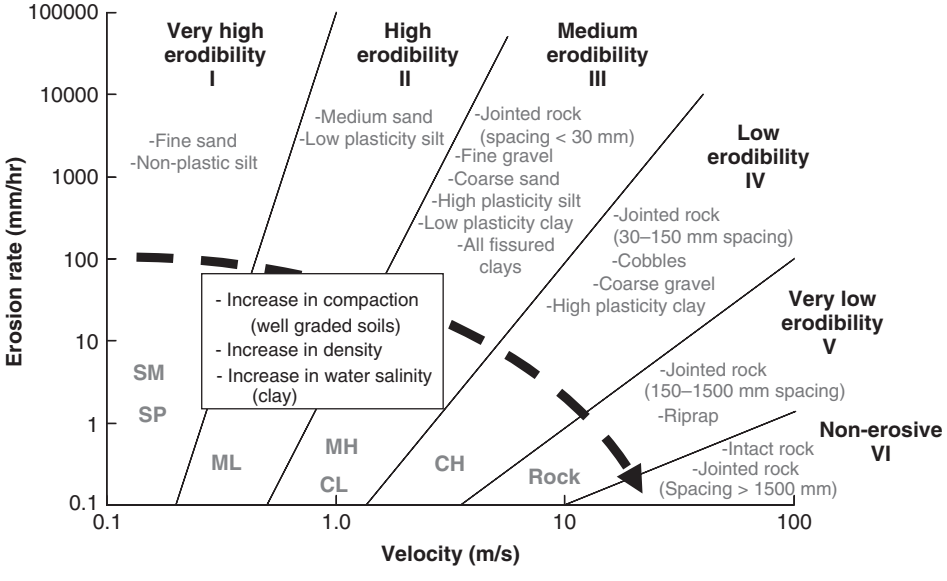

Figure 23.13s Proposed erosion categories for soils and rocks based on velocity.

Table 23.1s shows all the calculations and the contours of erosion after 2 hours and 72 hours of overtopping erosion are shown in Figure 23.14s.

Drop Height m	Velocity m/s	Erosion Rate mm/hr	Erosion Depth after 2 Hr m	Erosion Depth after 72 Hr m
0	0	0	0	0
0.06	1.1	0.1	0.0002	0.0072
1	4.43	6	0.0012	0.432
2	6.26	18	0.036	1.296
3	7.67	35	0.07	2.52
4	8.86	58	0.116	4.176
5	9.9	91	0.182	6.552

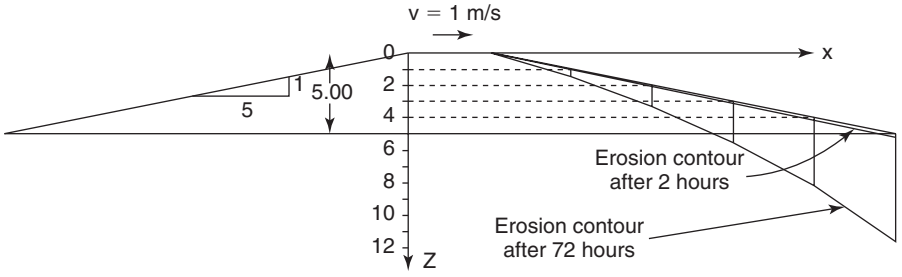

Figure 23.14s Contour of erosion after 2 and 72 hours.

Problem 23.11

Repeat problem 23.10 for a flood that lasts 72 hours.

Solution 23.11

Same approach but multiply by 72 hours instead of 2 hours.